MOLECULAR IMAGING AND BIOLOGY

Mol Imaging Biol (2019) 21:200–218
DOI: 10.1007/s11307-018-1239-2

Published Online: 25 June 2018

REVIEW ARTICLE

# Fluorescence Guidance in Surgical Oncology: Challenges, Opportunities, and Translation

Madeline T. Olson,[1,2] Quan P. Ly,[2,3] Aaron M. Mohs[2,4,5]

[1]*Eppley Institute for Research in Cancer and Allied Diseases, University of Nebraska Medical Center, Omaha, NE, 68198, USA*
[2]*Fred and Pamela Buffet Cancer Center, University of Nebraska Medical Center, Omaha, NE, 68198, USA*
[3]*Department of Surgery, University of Nebraska Medical Center, Omaha, NE, 68198, USA*
[4]*Department of Pharmaceutical Sciences, University of Nebraska Medical Center, 5-12315 Scott Research Tower, Omaha, NE, 68198, USA*
[5]*Department of Biochemistry and Molecular Biology, University of Nebraska Medical Center, Omaha, NE, 68198, USA*

**Abstract**

Surgical resection continues to function as the primary treatment option for most solid tumors. However, the detection of cancerous tissue remains predominantly subjective and reliant on the expertise of the surgeon. Surgery that is guided by fluorescence imaging has shown clinical relevance as a new approach to detecting the primary tumor, tumor margins, and metastatic lymph nodes. It is a technique to reduce recurrence and increase the possibility of a curative resection. While significant progress has been made in developing this emerging technology as a tool to assist the surgeon, further improvements are still necessary. Refining imaging agents and tumor targeting strategies to be a precise and reliable surgical strategy is essential in order to translate this technology into patient care settings. This review seeks to provide a comprehensive update on the most recent progress of fluorescence-guided surgery and its translation into the clinic. By highlighting the current status and recent developments of fluorescence image-guided surgery in the field of surgical oncology, we aim to offer insight into the challenges and opportunities that require further investigation.

**Key words:** Image-guided surgery, Optical surgical navigation, Surgical oncology, Fluorescence, Optical contrast agents

## Optical Surgical Navigation

### *Clinical Relevance*

With over 14 million estimated new cases, and 8 million deaths reported in the most recent *World Cancer Report*, cancer remains a leading cause of death across the globe [1]. In the United States alone, over 1.73 million new cases of cancer and over 600,000 deaths are estimated in 2018 [2]. Despite significant expansion and diversification of treatment options, surgical resection continues to serve as the cornerstone of treatment for most solid cancers. However, there are many complexities to tumor resections that require further investigation and/or improvement. Complete tumor resection relies on a surgeon's ability to differentiate between malignant and benign tissue using palpable and visual cues, but the infiltrative nature of cancerous tissue can make it difficult for surgeons to remove the entire tumor. The lack of differentiation, involvement of critical nerves and vasculature, and the stage of disease progression can complicate a tumor resection and lead to either incomplete removal or removal with significant morbidity [3]. If the tumor is not removed in its entirety, the residual cells at the surgical margin that result in positive margins, can lead to disease recurrence [4–6]. Fluorescence image-guided surgery (FIGS) offers a strategy to assist surgeons in delineating cancerous tissue through the use of fluorescence. Using

*Correspondence to:* Aaron Mohs; *e-mail:* aaron.mohs@unmc.edu

this technology to color code the surgical field would better equip surgeons with the visual information needed to remove the tumor in its entirety or abort if needed, avoid inadvertent injury to non-cancerous tissue, confirm cancerous lymph nodes and metastases, and decrease disease recurrence.

FIGS may not be an equally beneficial solution for all cancer types. For example, in both ovarian and pancreatic cancers, the disease is often highly advanced and metastatic upon detection [7, 8]. Only 20 % of pancreatic cancer patients are candidates for resection because of the aggressive dissemination of the disease and the high degree of involvement of the surrounding vasculature [9–12]. Of the pancreatic cancer patients who undergo surgical resection, 80 % of these patients will eventually succumb to the disease due to recurrence [8, 10]. In ovarian cancer, it is common that patients undergo debulking surgery to leave less than 1 cm of residual disease, but because of the advanced stage of the disease, adjuvant chemotherapy is often used in conjunction with resection in an attempt to ablate microscopic disease [7, 13]. However, like pancreatic cancer, most patients with ovarian cancer develop recurrent disease [14]. To make surgical resection a viable and curative treatment option for highly metastatic cancers such as these, the development of early detection biomarkers is essential.

In addition to highlighting the primary tumor, FIGS may play a critical role in detecting early peritoneal disease and preventing inadvertent damage to critical and healthy tissue. Fluorescent detection of early peritoneal disease can reduce the number of unnecessary subsequent surgeries required to remove undetected metastases [15, 16]. Nerve damage is a potential complication during surgical resection, especially in prostate and head and neck cancers, among others, because the fine innervations are difficult to differentiate from the tumor tissue. Damage to nerves during surgical resection can result in increased postoperative morbidity, including increased pain and impaired function [17, 18]. Extensive nerve identification during surgery often results in prolonged operation time and possible damage to surrounding tissue [19]. However, the use of FIGS has shown efficacy in labeling the nerves to avoid this type of injury during resection [17, 20–22].

## *Contrast Agents*

Contrast agents applicable to FIGS generally fall into two categories; either visible or near infrared (NIR) dyes. NIR dyes (~ 700–1000 nm) offer potential advantages compared to visible dyes because of increased depth of light penetration, decreased light scattering, and lower tissue autofluorescence in the NIR region [23]. The properties of NIR fluorophores provide the high signal to background ratio (SBR) required to aid surgeons in better differentiating cancerous tissue from normal tissue. Table 1 summarizes the properties of contrast agents that are frequently investigated for FIGS, including methylene blue, 5-aminolevulinic acid (5-ALA), cyanine-based dyes, including indocyanine green (ICG), IRDye800, and Dyomics dyes, and quantum dots. Fluorescein was an early dye used to illuminate tumors, but it is no longer as prevalent for FIGS because of its high autofluorescence and low tissue penetration [60]. Additionally, several cases have reported fluorescein causing anaphylactic shock [61, 62]. Each contrast currently used for FIGS comes with its own considerations, emission wavelength, quantum yield, toxicity, accumulation, and regulatory approval.

## *Methylene Blue*

Methylene blue is a widely utilized, FDA approved, visible wavelength dye [63]. This dye was developed as an alternative to its predecessor, isosulfan blue (Lymphazurin). Because there was a shortage of isosulfan blue when sentinel lymph node mapping was accepted as the staging modality for breast cancer and melanoma, methylene blue is now commonly used instead. Furthermore, there were reports of a 1–3 % incidence rate of anaphylaxis with isosulfan blue. There have been reports of anaphylactic shock with methylene blue, but the rate is much lower. Regardless, the use of this dye is limited during pregnancy, because of its teratogenic potential [30, 31]. Nevertheless, this contrast agent has many applications for FIGS, as well as photodynamic therapy for cancer [32]. Previous studies have demonstrated the efficacy of this dye in identifying vital structures such as parathyroid glands, nerves, and ureters, to avoid injury during cancer resection [33–37]. Additionally, methylene blue has been used to identify sentinel lymph nodes and the presence of certain tumors [38–42]. However, uptake of this dye is highly variable and dependent on tumor type. Methylene blue is further limited because it lacks the favorable properties of NIR dyes, and it requires a high dose for detection in order to overcome autofluorescence [63].

## *5-ALA*

5-ALA is a visible wavelength dye that was recently FDA approved for use as a fluorescent imaging agent in patients with high grade gliomas. A precursor molecule of the hemoglobin synthesis pathway, 5-ALA catalyzes the production and accumulation of the compound protoporphyrin IX (PpIX) in cancerous tissue. This compound exhibits fluorescence when excited by a violet-blue light source (405 nm), allowing for the visualization of cancerous tissue [24, 25]. The use of 5-ALA is associated with high specificity and positive predictive values [26]. However, while improved resection with 5-ALA correlates to improved survival rates, there are also limitations to the use of this contrast agent, particularly its inconsistency [27]. Visible fluorescence is uncommon in low grade gliomas, and thus the usage of 5-ALA guided resection is restricted to

solely higher grades. Previous studies have noted variance in the type of fluorescence, including both solid red fluorescence in the tumor tissue, and vague pink fluorescence at the transition zone between normal and cancerous tissue [28]. In areas of lower fluorescence, the ability of the dye to accurately identify cancerous tissue is sacrificed, thus poor sensitivity and low negative prediction values remain concerns for the use of 5-ALA [24, 26, 27, 29, 63].

### *ICG*

ICG is an FDA-approved NIR tricarbocyanine dye that has many uses in the clinic and expanding uses in FIGS. This dye has very low toxicity and has been approved for use in determining hepatic function, cardiac output, and ophthalmic perfusion for decades [43, 63]. ICG has also shown efficacy for FIGS in sentinel lymph node mapping, evaluating blood flow in reconstructed organs, and identifying and marking tumors for a variety of different solid cancer types [43–48]. Because ICG is a NIR dye, it can be detected more deeply in tissues , making it a good candidate for real-time FIGS. This dye is widely used across clinical trials and patient care settings, and has shown great potential for use with FIGS. However, ICG is limited by its aqueous instability, short circulation time, and concentration-dependent quenching. ICG also lacks the functional groups necessary for conjugation, rendering it a non-specific contrast agent. However, studies have shown that encapsulation of ICG improves its targeting abilities and circulation time, offering solutions to improve ICG for FIGS use [49, 50].

### *Dyes on the Rise*

While 5-ALA, methylene blue, and ICG are the most prominent dyes entering clinics and clinical trials, many other contrast agents are showing significant promise in the pre-clinical phases. Cyanine derivatives (*e.g.*, Cy7.5) and those developed by Dyomics (Jena, Germany) and LI-COR (Lincoln, NE, USA), quantum dots, and others have been adapted for FIGS use in preclinical investigations (Table 1). IRDye800 (LI-COR) is perhaps the most advanced, appearing in current clinical trials, particularly in conjugation with antibodies [51–53]. The use of cyanine dyes overall, however, is still mostly restricted to the laboratory, but the conjugatable nature, stability, and high fluorescent capabilities of these dyes suggest potential for further success and clinical translation in the future [57, 59]. Quantum dots have also demonstrated significant potential for use in bioimaging applications, but concerns with safety and toxicity, especially the release of heavy metal ions and generation of reactive oxygen species, need to be addressed [64]. Development of non-toxic and biocompatible quantum dots is the next step towards clinical translation [65].

### *Instrumentation*

FIGS is advantageous to other imaging modalities, such as x-ray computed tomography (CT) or magnetic resonance imaging (MRI), because it is less expensive, more mobile, and more feasible for integration into the surgical theater [66]. Additionally, FIGS provides surgeons with real-time intraoperative feedback. FIGS also lacks the ionizing radiation used in other imaging modalities and is seen as extremely safe for use with clinically approved contrast agents and probes [32]. A typical FIGS instrument has three main optical components: an excitation source, a collection source, and a display (Fig. 1). The excitation source must be able to excite the fluorophore at a working distance from the surgical field and emit a light that does not overlap with the emission wavelength of the fluorophore. Ideally, excitation light should be centered around the peak absorption wavelength for the fluorophore in use [67]. Common excitation sources are laser diodes, light-emitting diodes (LED), or filtered broadband lamps. Filtered broadband lamps are not ideal for image-guided surgery because they are inefficient. These lamps produce excessive heat and lose significant optical power on the surgical field. Additionally, many photons must be discarded in order to produce a narrow enough band of excitation [68–70]. Therefore, LEDs and laser diodes are preferential for use in FIGS. However, each of these comes with its own considerations as well. LEDs provide a compromise of adequate efficiency, spectral confinement, and cost. However, heat dissipation is also a concern for this type of excitation source [67]. Laser diodes are the most precise in terms of spatial and spectral

**Table 1.** Summary of select contrast agents for use in FIGS

| Fluorophore | Excitation/emission (nm) | Target | Applications in FIGS | Approval phase | References |
|---|---|---|---|---|---|
| 5-ALA | 405/635 | Non-specific | Glioma detection | FDA approved | [24–29] |
| Methylene blue | 665/686 | Non-specific | Vital structure detection, SLN, tumor detection | FDA approved | [30–42] |
| ICG | 80/822 | Non-specific | SLN, reconstruction, tumor detection | FDA approved | [23, 43–50] |
| IRDye800CW | 774/789 | Non-specific, conjugatable | Tumor detection and imaging | Clinical trials | [23, 51–53] |
| Dy800 | 777/791 | Non-specific, conjugatable | Tumor detection and imaging | Pre-clinical | [54–56] |
| Other cyanine dyes | Cy 5-658/666<br>Cy 5.5-679/696<br>Cy 7-747/774<br>Cy 7.5-788/808 | Non-specific, conjugatable | Tumor detection and imaging | Pre-clinical | [23, 57, 58] |
| Quantum dots | 700–1500 | Non-specific, conjugatable | Tumor detection and imaging | Pre-clinical | [23, 59] |

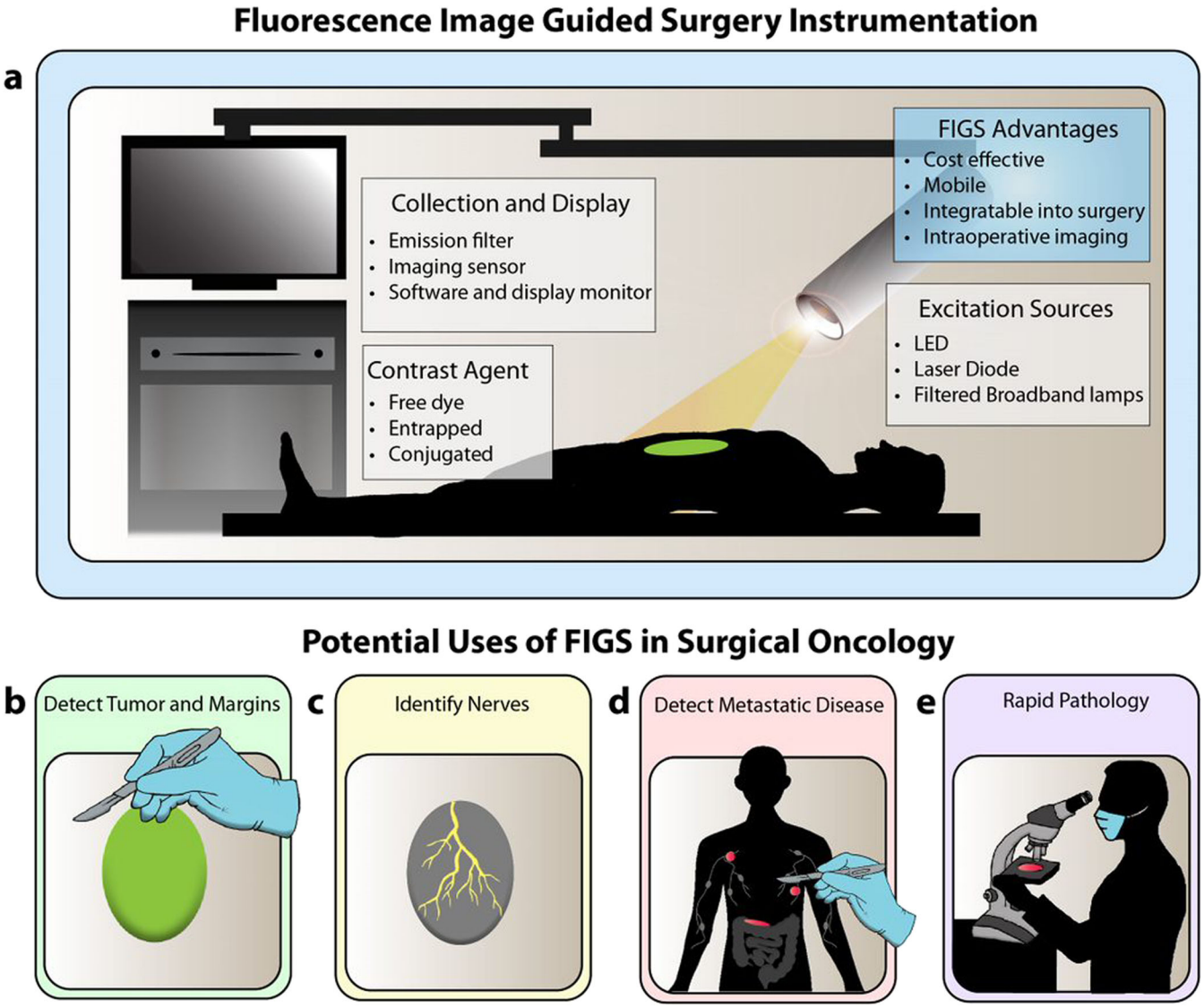


**Fig. 1** FIGS instrumentation and potential uses: **a** FIGS instrumentation consists of three critical components: an excitation source, a collection source, and a display. The excitation source is responsible for exciting the fluorophore, the collection source detects fluorescent emission and discards other light, and the display provides intraoperative real-time feedback of the surgical field. Contrast agents for FIGS can be used in several formulations, including free dyes, dyes entrapped in nanoparticles, and dyes conjugated to targeting moieties. FIGS has many potential uses in the field of surgical oncology. **b** Surgeons are able to detect tumors and tumor margins with FIGS, which can result in a reduction in recurrence. **c** Additionally, FIGS can be used to identify critical nerves during surgery, to avoid injurious resection. **d** FIGS has shown efficacy in detecting metastasis in addition to the primary tumor, especially lymph nodes. **e** Pathologists can use FIGS for rapid *ex vivo* analysis of tissue samples, to confirm negative margins.

confinement, but raise concerns in terms of safety and cost [66, 68]. The collection source plays a critical role in FIGS instrumentation in transmitting the NIR signal from the excited fluorophore to the camera for interpretation. The sensitivity of detection is greatly determined by the background signal. In order to achieve a high level of sensitivity for the NIR signal, the FIGS hardware must be able to filter out and minimize background light. Differences in hardware design and emission filtration techniques can play a critical role in limiting the background signal and improving the sensitivity of FIGS instrumentation. [68–70]. Display monitors are the most common form of image display that are used to integrate the NIR and surgical field images to provide real-time feedback to surgeons. Most current display monitors feature an image of the surgical field next to an image of the NIR region on the surgical field. Previous designs have suggested developing a more seamless integration by superimposing the NIR image onto the image of the surgical field [3]. A recent review by Dsouza *et al.* extensively compares current FIGS instrumentation systems and their efficacy, as well as features of FIGS systems that are most valued for clinical implementation. Increasing

sensitivity to low contrast agent concentrations, obtaining quantification of fluorophore concentration, and adapting to multi-fluorophore imaging capabilities, are important considerations for FIGS instrumentation development [69].

## Tumor Targeting Strategies—Passive

### *Selective Accumulation*

The strategy of passive targeting was derived from the observation that certain macromolecules preferentially accumulate in tumors [71–73]. Passive targeting for the delivery of both free and conjugated contrast agents for FIGS exploits the enhanced permeability and retention (EPR) effect to provide selective and preferential accumulation of contrast agents in tumor tissue, as shown in Fig. 2. The biological basis for this phenomenon stems from the unique properties of vasculature and lymphatics in the tumor microenvironment. As tumors increase in size, inadequate delivery of oxygen and vital nutrients create a hypoxic environment in the center of the tumor. This hypoxic condition induces the expression of angiogenic growth factors to form neovasculature that will support the rapidly proliferating cells [74]. However, the architecture of this new vasculature is irregularly dilated, highly disorganized, and hyper-permeable [75–77]. A loosened association between pericytes and endothelial cells further contributes to the vascular abnormality and hyper-permeability [78]. In addition to faulty vasculature, poor lymphatic distribution and the markedly impaired lymphatic drainage in the tumor [79, 80] create a retentive tumor environment that can potentially be utilized in FIGS due to the deposition of contrast agents in the tumor tissue [81, 82].

### *Challenges to Implementation*

Despite its proposed efficacy, there are many challenges involved with the implementation of EPR as a potential mechanism for contrast agent delivery. One criticism of this method of delivery is its relatively modest results, suggesting less than a twofold increase in delivery to tumor tissues in comparison to normal tissues [83, 84]. Because of the heterogeneity of tumors, it is difficult to predict the extent of the EPR in a specific patient. Tumor size, location, and organ type all play a role in the magnitude and presence of the EPR effect. While the unique characteristics of the tumor microenvironment are credited for the generation of the EPR effect, the same biological factors can significantly impede the efficacy of the phenomenon. For example, as depicted in Fig. 2b–e, heterogeneous perfusion, gradients of tumor cell growth, stress from the tumor stroma (including fibroblasts, mesenchymal cells, and immune cells), and high interstitial fluid pressure can contribute to the impediment of contrast agent delivery [83–85]. Tumor vasculature abnormalities often result in areas of poor and heterogeneous perfusion throughout the tumor. While the leaky tumor vasculature may contribute to contrast agent retention, heterogeneous blood flow can impede the homogenous delivery of contrast agents in the tumor tissue [85]. These variations in blood supply also lead to obscure gradients in tumor cell growth. While tumor cells proliferate rapidly near the vasculature, proliferation decreases at sites distant to the vasculature. The high density of proliferating cells surrounding the vasculature can compress blood vessels and lymphatics, preventing the convection of contrast agents in certain regions of the tumor [86–88]. Increasing density of tumor cell growth combined with poor lymphatic drainage result in very high interstitial pressure inside of the tumor. While the dense tumor center has a very high interstitial fluid pressure, there is a significant drop in pressure at the tumor periphery, which may result in the leakage of contrast agents into the peritumoral tissue [85, 89, 90]. The dense extracellular matrix of the tumor stroma further amplifies the solid stress in the tumor, constructing a collagen-rich network that hinders uniform contrast agent deposition [84, 85, 91]. Given the extent of the biological barriers, the EPR must be validated and improved upon. Otherwise, insufficient and unpredictable contrast agent delivery may render passive targeting an obsolete strategy for FIGS.

### *Proposed Strategies for Improved Implementation*

While there is significant controversy surrounding the prevalence and usefulness of the EPR effect, current research has demonstrated potential strategies to reorganize the tumor microenvironment to improve the EPR as well as use the presence of the EPR as a biomarker. Microenvironment alteration strategies include modifying tumor vasculature and blood flow, increasing vascular permeability, modulating the tumor stroma, and killing cancer cells [83, 84, 92–94]. Isolating biomarkers for the presence of the EPR effect has also been suggested to identify potential candidates for receiving nanotherapeutics and passive delivery of contrast agents [95–97]. The implications of the EPR in personalized medicine, as well as the regulatory appeal, recognize the potential and translational importance of the EPR effect. Compared to highly specific targeted probes, passive targeting *via* the EPR effect is advantageous in its use of generic fluorescent probes, such as methylene blue and ICG. These agents have already been approved for use in the clinic, whereas targeted probes have yet to see regulatory approval [98]. Despite the significant barriers to implementation of the EPR effect as a delivery strategy for FIGS, current research has validated the potential for strategic improvements and clinical translation of utilizing the effect.

## Tumor Targeting Strategies—Active

The strategy of active targeting in FIGS is based on the recognition of a fluorescent moiety conjugated ligand by its

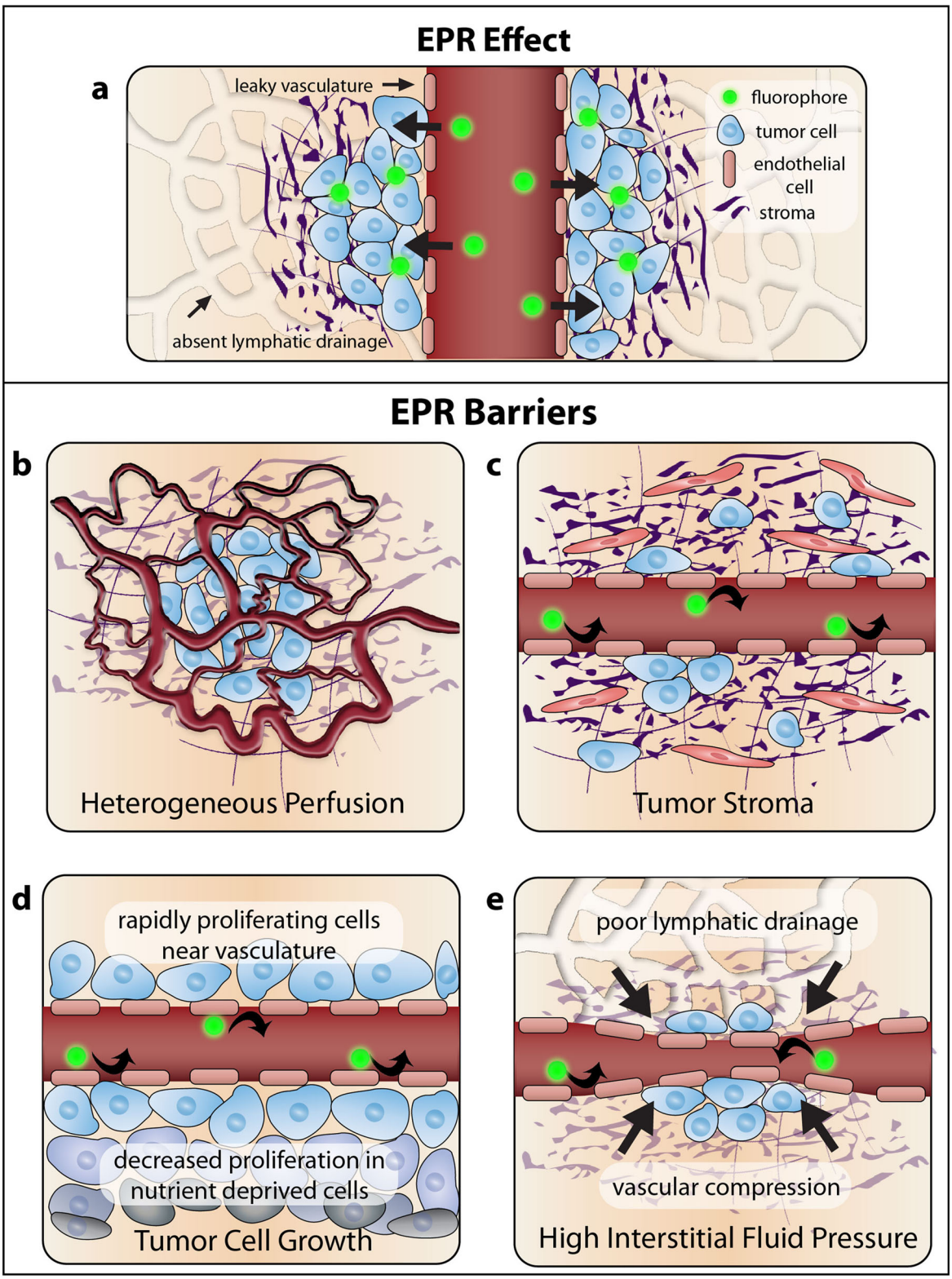


**Fig. 2** Passive targeting mechanisms and barriers: **a** the strategy of passive targeting for FIGS is based on the enhanced permeability and retention effect in tumors. Contrast agents enter the tumor through the leaky vasculature and stay in the tumor because of poor drainage. However, there are many barriers to the efficacy of this targeting strategy. **b** Heterogeneous perfusion from abnormal vasculature can result in inadequate perfusion in some areas of the tumor. **c** The presence of a dense tumor stroma can prevent penetration of contrast agents. **d** High gradients of tumor cell growth near to the vasculature can increase pressure and prevent contrast agents from leaking into the tumor. **e** High interstitial fluid pressure from inadequate lymphatic drainage can also prevent contrast agent deposition.

target receptor on a tumor. This technique harnesses the unique microenvironment of a tumor, focusing on using ligands to target differentially expressed proteins in tumors for increased, and more precise contrast agent delivery. The accessibility of the tumor receptor and its level of expression are important factors to consider in active targeting. Ligands used to target the overexpressed receptor on the tumor should have a high binding affinity and low toxicity, exhibit high specificity, and present groups for conjugation to a contrast agent for imaging [99]. As shown in Fig. 3, antibodies, antibody fragments, proteins, peptides, aptamers, small molecules, and nanoparticle conjugates are examples of commonly used ligands used to target tumor receptors for FIGS. While active targeting probes may achieve a higher degree of specificity for the tumor target than passive targeting, background noise and non-specific binding still occur, suggesting the need for further improvement. High background noise and non-specific binding can significantly limit the detection capabilities of FIGS, inhibiting the surgeon's ability to differentiate cancerous tissue and metastatic lesions. The pharmacokinetic properties of the probe are a contributing factor to the background noise and non-specific binding. Many dyes that are used for FIGS are cleared from the body through the liver, which can result in a high level of background signal in the gastrointestinal tract. Further investigations to reduce background noise, as well as non-specific binding, are important for improving the accuracy and signal of FIGS [100]. Finally, one of the biggest limitations of FIGS is that it lacks the ability to image preoperatively in most cases, and it cannot image at all clinically relevant depths. It is essential to continue developing active targeting methods that can functionally integrate preoperative and intraoperative imaging, as well improve the SBR for FIGS.

## *Antibodies and Antibody Derivatives*

The use of antibodies as a FIGS targeting strategy is widely investigated and, while the vast majority of these investigations for FIGS are pre-clinical, several antibody–fluorophore conjugates are in clinical trials [101–104]. Cetuximab and panitumumab, targeting human epidermal growth factor receptor (EGFR), and bevacizumab, targeting vascular endothelial growth factor (VEGF), are common antibodies used for fluorescence imaging in current clinical trials for a variety of different cancers (NCT02583568, NCT02415881, NCT03134846) [53, 105]. In addition to imaging, antibodies have the potential to be a useful tool for diagnostics, therapeutics, and drug delivery. However, the pharmacokinetic requirements differ for each of these uses [106, 107]. For instance, slow circulation is preferential for therapeutic

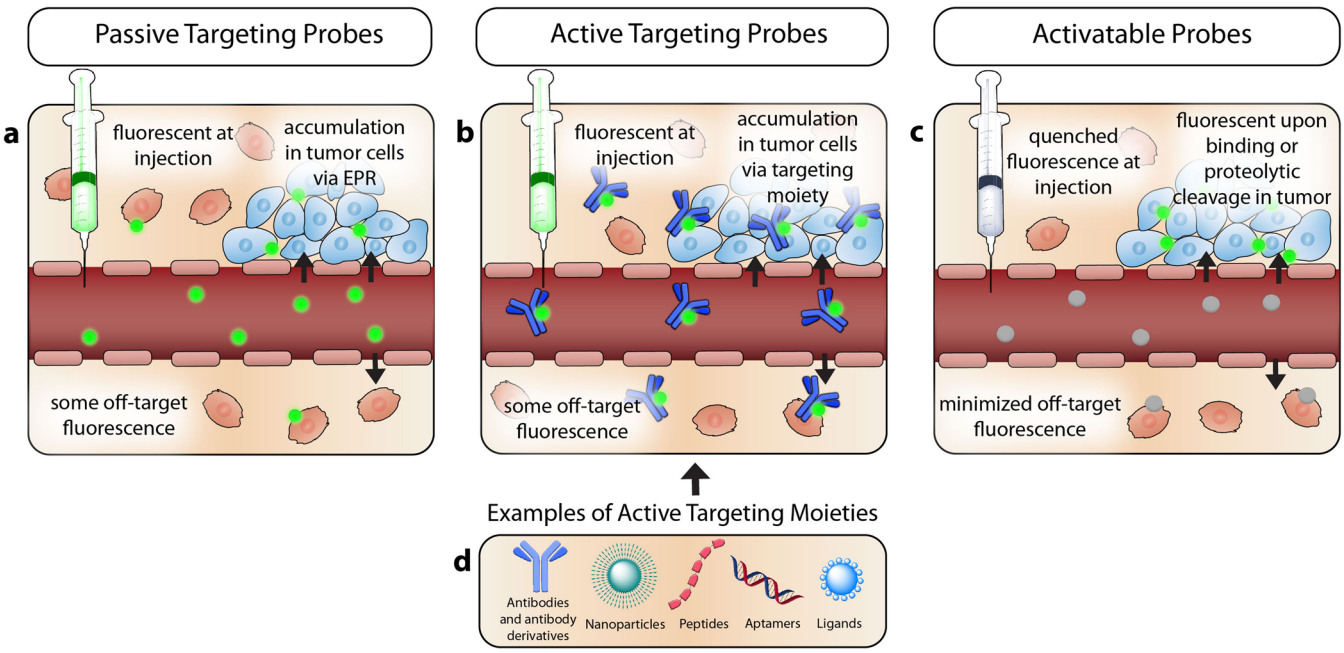


**Fig. 3** Tumor targeting strategies: **a** passive targeting relies on the selective accumulation of contrast agents in the tumor tissue, *via* leaky vasculature and absent lymph drainage. The contrast agents used in this targeting strategy are fluorescent at injection and can result in non-specific binding when the contrast agent is deposited outside the confines of the tumor. **b** Active targeting probes rely on a targeting moiety conjugated to a contrast agent to specify fluorescence. **c** Activatable probes exhibit quenched fluorescence when they are injected or topically applied. Binding to specific antigens or cleavage by a tumor protease results in the activation of these probes. Therefore, only cells that are targeted fluoresce. **d** There are many moieties available to use for active targeting, including but not limited to antibodies, antibody derivatives, nanoparticle scaffolds, peptides, ligands, and aptamers.

antibodies, but fast clearance is necessary for imaging purposes. Therefore, dual function antibody probes must balance the requirements for its desired function. The binding sites of antibodies can be modified to achieve high specificity for a given target, a favorable trait for an imaging agent. However, antibodies have limitations in FIGS. This is in part due to their large size (~ 150 kDa) and long circulation time, resulting in impaired tumor penetration and increased background signal during imaging. Engineered antibody fragments provide a compromise to full antibodies. Fragments are smaller in size (25–100 kDa), and therefore have faster clearance and decreased background signal during imaging, but sacrifice the extent of tumor uptake. These fragments have shown efficacy in recent studies of prostate cancer [108, 109]. Nanobodies and affibodies have also shown efficacy as alternatives to full antibodies. Affibodies, tiny protein scaffolds, are an advantageous alternative to full antibodies because of their small size (2–20 kDa) which allows for deeper tissue penetration, as well as their fast circulation time. These characteristics, in addition to their cheaper cost, make affibodies an excellent candidate for imaging [110, 111]. An IRDye800CW labeled synthetic affibody, ABY-029, has recently demonstrated success in preclinical studies for labeling EGFR-positive regions in gliomas and is currently undergoing microdosing clinical trials for multiple cancer types [112, 113]. Nanobodies (~ 12–15 kDa) are typically constructed from the variable region of an antibody's heavy chain. The advantages of nanobodies are similar to affibodies in many regards, featuring high penetration and targeting, and rapid clearance [114, 115]. Recent trends in antibody-based targeting strategies for FIGS may favor the smaller fragments and derivatives of antibodies rather than their fully assembled parents because of their increased compatibility with imaging requirements.

## *Peptides*

Peptides are linear or cyclic amino acid chains linked by peptide bonds. This type of probe is advantageous as an imaging agent because of rapid distribution, small size, ease and scalability of synthesis, specificity, and stability [116]. Despite their many advantages, peptides must be optimized in order to demonstrate translational potential. Their short half-life and degradation may prevent peptides from reaching their target. To combat this, peptides can be chemically modified to slow renal clearance and increase target affinity. Methods for modifying peptide probes for FIGS has been previously described [117]. There are a wide variety of peptides being investigated in laboratory settings including Arg-Gly-Asp (RGD), somatostatin (SST), gastrin releasing peptide (GRP), and neurotensin (NT) among many others. In a recent study, a cyclic RGD-ZW800-1 was investigated as a generic tracer for multiple cancer types and proved to be efficacious for both tumor and ureter identification [118]. The use of a zwitterionic dye such as ZW800 can overcome problems with background noise in FIGS. Because this dye is eliminated through renal filtration rather than liver clearance, studies have shown improved SBR and decreased background noise, especially in the gastrointestinal tract [100, 119]. Neurotensin conjugated to IRDye800 also showed value as a fluorescence imaging agent for potential use in screening pancreatic cancer patients [120]. Another peptide probe of recent interest is the pHLIP derived probe, or the pH low insertion peptide probe. This targeting strategy utilizes the characteristic acidic pH found in the tumor environment. The probe is designed so that upon sensing a change in pH, the probe is protonated and becomes more hydrophobic, thus folding and forming a transmembrane helix inserted in the membrane of the cancerous cells [121]. Recent studies have employed this technology for detecting bladder cancer and improving fluorescence signal in a breast cancer model [122, 123].

## *Aptamers*

Aptamers are single-stranded DNA or RNA sequences that are capable of binding to targets by forming three-dimensional structures. Aptamers are typically selected *in vitro* using a method called systematic evolution of ligands by exponential enrichment (SELEX), as well as variations on this technology. Explanations of aptamer selection using these libraries have been previously described [124, 125]. Aptamers have shown great potential for serving as a targeted probe for FIGS imaging because of the small size (5–40 kDa), ease of synthesis and modification, wide range of targets, and stability. Drawbacks to using these sequences as targeting agents for FIGS are that aptamers are regularly degraded by nucleases, and not all aptamers have a high binding affinity. This can result in weak signal generation for imaging. However, this can be improved upon by using scaffolds, such as nanoparticles or quantum dots, to improve the binding affinity of the aptamer, thus providing increased specificity and enhanced signal [126]. A recent study demonstrated the efficacy of aptamer conjugated quantum dots for identifying margins in glioma by binding to EGFR variant III on the tumor cell surface [127]. A different study employed the use of silica based nanoparticle and aptamer conjugate to act as a theranostic agent to image and inhibit tumor angiogenesis [128]. Beyond FIGS, aptamers have shown great potential for use in a variety of applications, especially in drug delivery. Aptamers are prevalent in clinical trials, but not yet in relation to FIGS. Most of the current clinical trials investigate aptamer use in macular degeneration, though recently posted clinical trials propose identifying aptamers to identify biomarkers in bladder cancer (NCT02957370), as well as using a Ga-68 aptamer conjugate to test its

diagnostic capabilities in positron emission tomography (PET)/CT (NCT03385148).

### *Ligand-Based Targeting*

There are several ligand-based targeting strategies that are typically used to functionalize and specialize the surface of nanoparticles. Two commonly explored examples of this strategy include proteins like transferrin and small molecules such as folic acid. Small molecules are advantageous as a targeting strategy because of their size, cost, and stability. However, they are scarce because of the difficulty of finding a ligand and the intense screening process involved [72, 129]. These molecules are typically used to functionalize the surface of nanoparticles for more specific targeting. Folic acid is perhaps the most common example of a small molecule used in the literature. Folic acid conjugated quantum dots has proved successful as a theranostic agent in human cervical carcinoma cells [130]. Additionally, OTL38, a folate receptor targeted contrast agent, has shown success in multiple cancer models [131, 132]. A recent study used a folate targeted contrast agent to identify lung cancer in large animal models [133]. Protein ligand-based strategies, such as transferrin, are advantageous in their specificity but present problems because of bulk and ability to trigger an immune response. A recent study implicated the use of holo-transferrin ICG nanoassemblies for imaging and photothermal therapy in gliomas [134].

### *Improving Active Targeting*

Despite the wide variety of targeting ligands explored in preclinical studies, there are still many limitations to active targeting for FIGS. While active targeting exhibits increased specificity of the probe for its target, non-specific binding still occurs, as shown in Fig. 3. Active probes constantly emit fluorescence with excitation, regardless of their proximity to the target, producing elevated background noise in FIGS [135, 136]. Additionally, off-target binding can occur if the targeted receptor is expressed in non-cancerous tissues. While each type of targeting strategy has its own strengths and weaknesses, there are several widely adapted strategies to improve the efficacy of these probes, including the use of nanoparticles and activatable probes. Nanoparticles may play a significant role in FIGS, especially in acting as a scaffolding system for many of the aforementioned targeting strategies. The large surface area to volume ratio of nanoparticles provides a large area to attach a wide range of targeting moieties. However, the long-term effects of nanoparticle administration are still not fully understood. Biocompatibility, biodegradability, and toxicity properties must be carefully considered on a case-to-case basis [137]. Nanoparticle size, shape, charge, and hydrophobicity can all influence the conjugation with a ligand [72]. Using a nanoparticle as a scaffold for a targeting ligand allows for multiple interactions and thus increased specificity with the target. Nanoparticle entrapped dyes have shown enhanced fluorescence and tumor contrast, and nanoparticles are effective carriers for drug delivery [49]. Previous studies have also shown that careful modification of nanoparticle size and surface coating can alter their biodistribution to favor renal filtration, allowing for increased SBR and decreased background noise [138]. Further investigation of nanoparticle modifications to alter the pharmacokinetic properties has the potential to improve the detection capabilities of FIGS. Given their functionality, current research for FIGS has demonstrated increased use of nanoparticles for more effective delivery, as well as brighter contrast.

There are two main categories of active targeting probes: “always on” probes and “activatable” probes. Activatable probes offer several advantages over probes that are always on, such as higher contrast, lower background noise, and improved sensitivity. As shown in Fig. 3, the fluorescent properties of these probes remain quiescent until they receive a signal to fluoresce, such as enzymatic cleavage or cellular internalization. Probes such as these that are activated by biomolecules in the local tumor environment have the potential to overcome some of the pitfalls of FIGS, such as background noise and low SBR, by eliminating non-specific binding and subsequent off-target fluorescence. Difficulties with implementation of these probe types depend on the specifics of the probe. High molecular weight activatable probes cannot be sprayed onto the surface of the tumor and must be injected intravenously. It may take days for the necessary tumor to background ratio to be achieved. Molecular binding-based activatable probes are typically conjugated to an antibody and are therefore significantly large in size. However, enzymatic activity controlled probes can be small in size, and therefore some can be applied with a spray [135]. The use of a matrix metalloprotease and γ-glutamyltranspeptidase as agents for inducing probe enzymatic cleavage and activating fluorescence has been recently explored for cancer detection [139].

Many of the aforementioned active targeting mechanisms have potential applications in the field of drug delivery, as well as FIGS. For instance, antibody–drug conjugates are being utilized in both preclinical studies as well as early and late stage clinical trials. These studies have shown increased ability to target diseased cells and increased antitumor potency [140–143]. Peptide and aptamer-based delivery systems have also shown efficacy in reducing off-target effects and increasing drug delivery to the tumor [144–146]. Therefore, there is an opportunity for parallel development of imaging probes and drug delivery systems that target the same receptor or biomarker. Furthermore, there is an opportunity to improve active targeting by incorporating multimodality imaging probes. One of the biggest limitations with FIGS is that it can only be used intraoperatively and cannot be used for preoperative planning. However, multimodal active targeting probes that use FIGS in

conjunction with MRI, PET, photoacoustic imaging, or CT can potentially improve preoperative detection and intraoperative resection [147–155]. Current multimodal probes employ many of the active targeting strategies to achieve a high level of accuracy for proving delivery and overcome some of the limitations of single modality active targeting.

While the variety of targeted probes continues to expand in versatility and function, regulatory restrictions are a significant consideration to successful implementation into clinical settings. In addition, each type of probe comes with its own set of developmental difficulties. Given the wide successes of different types of probes in the laboratory, it seems that there is not one type of probe that exceeds all others in terms of clinical potential. Instead, the functional imaging and targeting requirements should dictate the type of probe used, as each carry its own advantages. Further toxicity and feasibility studies, as well as appearance in clinical trials are needed to progress targeted probes for FIGS into the clinic.

## *In Vivo Versus Ex Vivo* Imaging

Surgical resection of tumors typically consists of three components. The primary tumor is assessed before the initial resection, the surgical margin is analyzed for remaining tumor, and the surgical field is assessed for regional metastasis [156]. As mentioned previously, remaining tumor at the surgical margin can result in disease recurrence. There are several strategies available to analyze the surgical margin for the presence of microscopic disease to achieve negative margins. Two common methods for intraoperative pathological examination of the surgical margin include intraoperative frozen section analysis (IFSA) and imprint cytology. Both methods have demonstrated reduced rates of positive margins after surgery, but the technology has limitations. IFSA, the current gold standard in margin detection, is highly variable in terms of sensitivity, and requires confirmation of negative margins on multiple tissue samples by a pathologist, which can add significant time onto the surgical procedure [157–159]. Imprint cytology is a faster and more

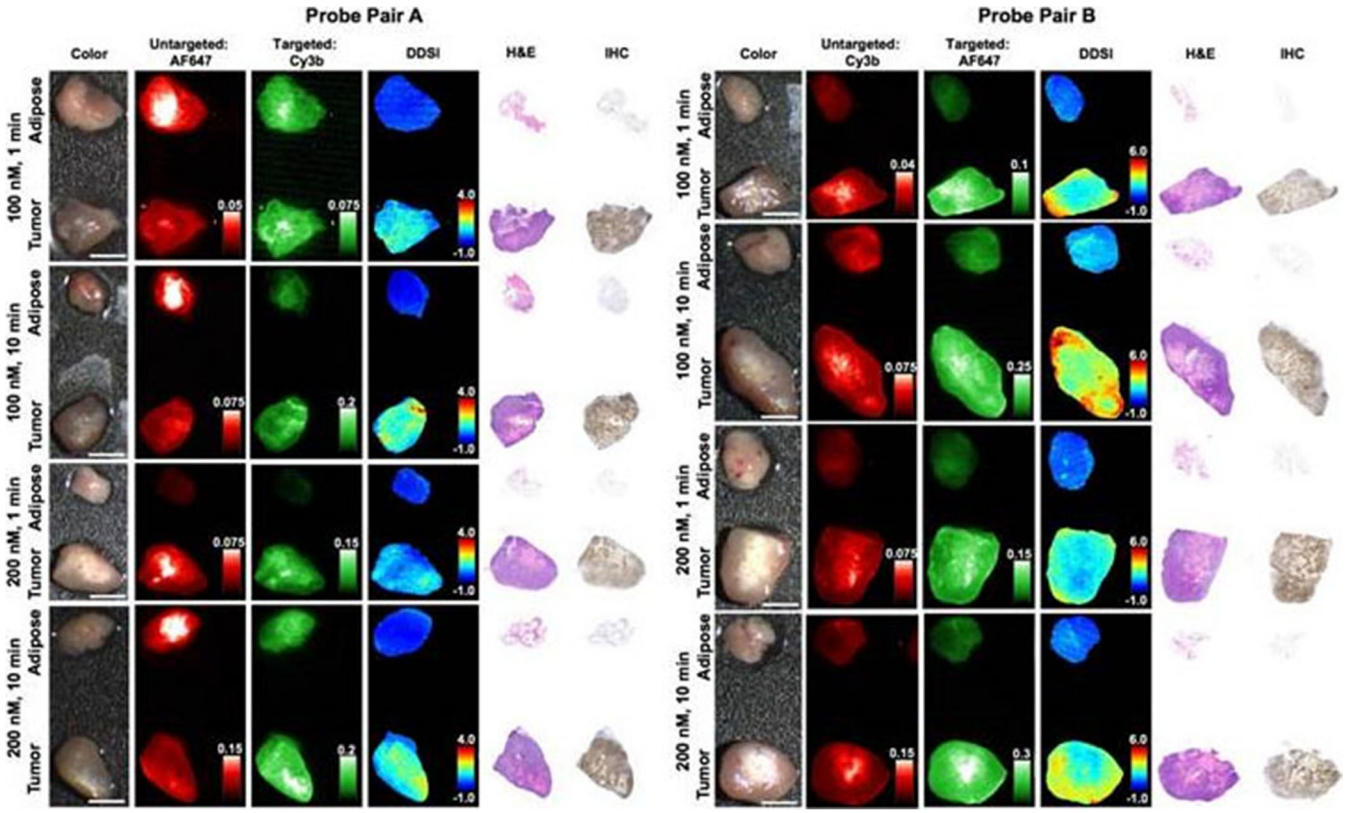


**Fig. 4** Dual probe *ex vivo* specimen imaging: representative color, fluorescence, DDSI (dual probe difference specimen imaging), H&E, and HER2 targeted IHC images of tumor and adipose tissue pairs following staining using a range of dual-stain soak concentrations and incubation times for **a** probe pair A (Herceptin-Cy3b, DkRb-AF647) and **b** probe pair B (Herceptin-AF647, DkRb-Cy3b). All images are representative of data collected for $n = 6$ tumor and adipose tissue pairs per staining condition. All untargeted and targeted channel images are background corrected, normalized by their exposure time and calibration drop intensity. DDSI images are displayed with equivalent color scales across staining conditions. H&E and IHC images were acquired from serial sections of the same tissue face imaged in the whole specimen DDSI images. H&E, hematoxylin and eosin; IHC, immunohistochemistry. Scale bars = 5 mm. *(Adapted from Barth CW, Schaefer JM, Rossi VM, Davis SC, Gibbs SL. Optimizing fresh specimen staining for rapid identification of tumor biomarkers during surgery. Theranostics 2017; 7(19):4722–4734. © Ivyspring International Publisher, 2017.)*

**Table 2.** Representative clinical trials utilizing FIGS

| | Objective | Trial identification | Cancer type |
|---|---|---|---|
| Indocyanine green (ICG) | Lymph node detection | NCT03297957 | Head and neck |
| | | NCT02840617 | Prostate |
| | | NCT02068820 | Endometrial |
| | | NCT01562106 | Endometrial |
| | | NCT02209532 | Endometrial, uterine, cervical |
| | | NCT02131558 | Endometrial |
| | | NCT03321448 | Cervical |
| | | NCT01818739 | Endometrial |
| | | NCT02478138 | Head, neck, oral |
| | | NCT02168452 | Breast |
| | | NCT01673022 | Endometrial, cervical |
| | | NCT02316795 | Breast, melanoma |
| | | NCT02119858 | Prostate |
| | | NCT02869152 | Rectal |
| | | NCT02850783 | Colon |
| | | NCT02423148 | Lung |
| | | NCT02817334 | Breast |
| | | NCT03320772 | Cervical |
| | | NCT02419807 | Breast |
| | | NCT01926743 | Gastric |
| | Tumor detection | NCT02611245 | Lung, esophageal |
| | | NCT02027831 | Head and neck |
| | | NCT01281488 | Renal |
| | | NCT01738217 | Liver |
| | | NCT02473159 | Breast |
| | | NCT02479997 | Breast |
| | | NCT02172989 | Breast |
| | | NCT02032485 | Colon |
| | Surgical reconstruction | NCT02629029 | Head and neck neoplasms |
| 5-ALA | Tumor detection | NCT01837225 | Breast |
| | | NCT03058705 | Bladder |
| | | NCT00285701 | Colon (dose finding) |
| | | NCT00752323 | Brain and CNS (dosing) |
| | Spatial correlation and modality agreement | NCT00870779 | Brain |
| IRDye800CW | Localization, safety, detection | NCT01508572 | Breast |
| | Signal detection | NCT03282461 | Head and neck |
| | | NCT01972373 | Rectal |
| | | NCT03154411 | Soft tissue sarcoma |
| | | NCT03134846 | Head and neck |
| | | NCT02129933 | Esophageal |
| | | NCT02583568 | Breast |
| | Dose/safety and detection | NCT03384238 | Pancreatic |
| | | NCT02901925 | Glioma |
| | | NCT02497599 | Renal |
| Other | OTL38 safety and detection | NCT02872701 | Lung |
| | | NCT03180307 | Ovarian |
| | SGM-101 safety and detection | NCT02973672 | Colon, rectum, pancreas |
| | LUM015 safety and Detection | NCT02438358 | Breast |
| | | NCT03321929 | Breast |
| | | NCT02584244 | Gastrointestinal |
| | | NCT03441464 | Prostate |

Search terms: "fluorescence imaging"
Exclusion criteria: withdrawn, terminated, suspended clinical trials

cost-effective method of analysis in comparison to IFSA. However, it also has variable levels of sensitivity and has a high probability of false-negative results [160]. The use of fluorescence imaging is increasingly being considered as an alternative method of histological analysis. Typically, FIGS is associated with intravenous administration of contrast agents for tumor detection, as the advantages of intraoperative real-time feedback of the surgical field are evident. However, significant investigations of fluorescent probe toxicity, dosage, optimal imaging time, and accuracy of molecular targeting must be conducted and approved before this technology can become the standard of care for eligible cancer patients. As an alternative use of FIGS, recent studies have demonstrated the use of *ex vivo* contrast agent administration to perform real-time fluorescence-guided histology [38, 161–163]. This technique lacks some of the intraoperative advantages such as preventing excessive tissue resection, but avoids some of the rigorous regulatory approval and testing, while still providing critical feedback on margin and nodal status. *Ex vivo* techniques are particularly useful for sentinel lymph node and positive margin detection. This strategy is efficacious and avoids

extended operating time and potentially re-excision. A recent study employed dual probe difference specimen imaging to differentiate between tumor and benign tissue using both a targeted and a non-targeted probe, as shown in Fig. 4 [161]. *Ex vivo* analysis provides an opportunity to utilize many of the targeted probes being developed in the laboratories into the clinic without extensive regulatory hurdles.

## Clinical Translation

The number of new clinical trials involving FIGS has increased dramatically over the past decade [164]. The adoption of target-specific probes and NIR dyes requires strict regulatory review to ensure patient safety. To fulfill these regulatory requirements, many current clinical trials are centralized around investigating the safety and efficacy of the FIGS agents. Endpoints to developing successful contrast agents, devices, and procedures need to be well defined in order to see faster progress of FIGS into patient care [165]. Current clinical trials for FIGS vary widely in terms of contrast agent, device, ligand conjugation, and objective, as shown in Table 2. ICG remains the most prominent contrast agent used in clinical trials, which is unsurprising due to its low toxicity and current FDA approval status. ICG is also significantly less expensive than other available contrast agents. SLN detection is currently under investigation for many cancer types, and there are some intriguing implementations of new technology. For example, in a fluorescence imaging study for SLN detection in head and neck cancer, the use of a hands free goggle system is being explored as an alternative to traditional monitor display FIGS devices as shown in Fig. 5 (NCT03297957) [166, 167]. IRDye800 has become another prominent contrast agent on the clinical trial stage. Many studies utilizing IRDye800 are investigating dosage, safety, and efficacy (NCT03384238, NCT02901925, NCT02497599). This dye is used in conjugation with several different antibodies across the spectrum of clinical trials, allowing for theoretically more precise tumor localization. Besides antibody conjugated IRDye800, there are several clinical trials studying IRDye800 conjugated to peptides. Recently a synthetic protease activated peptide dye conjugate entitled AVB-620, has entered a phase 2 trial for tumor and lymph node detection. Additionally, an anti-EGFR IRDye800 labeled affibody peptide has entered a phase 0 trial microdose study for signal detection in patients with recurrent gliomas (NCT02901925). In addition to ICG, IRDye800, and 5-ALA fluorescent dye based imaging agents in clinical trials, several other investigational probes have shown potential as prominent candidates for FIGS and cancer detection. The folate-receptor targeted fluorescent moiety, OTL38, has become a successful active targeting probe in clinical trials. A phase 2 study is currently underway, to investigate the ability of this imaging probe to aid in the detection of pulmonary nodules, as well as study the safety and tolerability of a single dose of this imaging agent (NCT02872701). The OTL38 probe is also being investigated in a phase 3 study to detect folate receptor positive lesions in ovarian cancer during cytoreduction,

**Fig. 6** Multimodal applications of FIGS: **a***in vivo* NIR fluorescence images after intravenous injection of free ICG and DOX@GdMSNs-ICG-TSLs in tumor-bearing mice at 2, 6, 12, 24, and 48 h, and the corresponding fluorescence images of different tissues after treated with free ICG and DOX@GdMSNs-ICG-TSLs at 24 h. **b** Relative fluorescence intensity of ICG in major organs induced by 808 nm laser (1.5 W/cm$^2$) irradiation at 24 h after i.v. administration. **c** US and PA images of DOX@GdMSNs-ICG-TSLs at various concentrations of ICG. **d** PA images of tumor-bearing mice after 6 and 24 h intravenous injection *via* tail of free ICG and DOX@GdMSNs-ICG-TSLs, respectively. **e** PA intensity of tumor sites after treatment with free ICG and DOX@GdMSNs-ICG-TSLs at 6 and 24 h. **f** T1-weighted MR images (7 T, spin–echo sequence; repetition time, TR = 500 ms; echo time, TE = 14.92 ms) of DOX@GdMSNs-ICG-TSLs nanoparticles at various Gd concentrations. And T1-weighted MR images of tumor-bearing mice before and after injected with DOX@GdMSNs-ICG-TSLs for 24 h. **g** Relative MR intensity before and after injecting DOX@GdMSNs-ICG-TSLs. Data are presented as means ± SD ($n = 5$); $^*P < 0.05$, $^{**}P < 0.01$. *(Adapted with permission from Sun Q, You Q, Wang J, et al (2018) Theranostic nanoplatform: triple-modal imaging-guided synergistic cancer therapy based on liposome-conjugated mesoporous silica nanoparticles. ACS Appl Mater Interfaces© 2018 American Chemical Society.)*

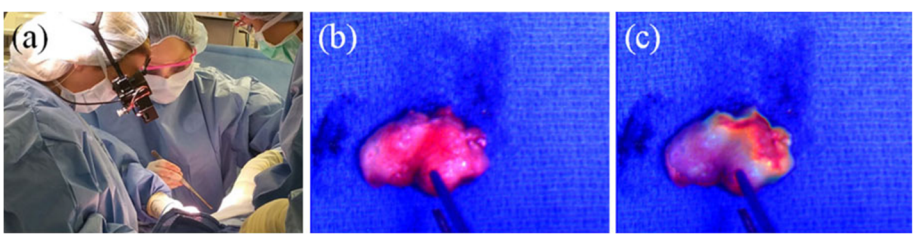


**Fig. 5** Goggles used for FIGS and cancer detection: fluorescence-guided SLN biopsy. **a** The surgeon wearing the goggles during SLN visualization in a breast cancer patient. **b** The color image of the excised SLN. **c** The superimposed color-fluorescence image of the excised SLN as seen by the surgeon. *(Adapted with permission from Mondal SB, Gao S, Zhu N, et al (2017) Optical see-through cancer vision goggles enable direct patient visualization and real-time fluorescence-guided oncologic surgery. Ann Surg Oncol 24:1897–1903.)*

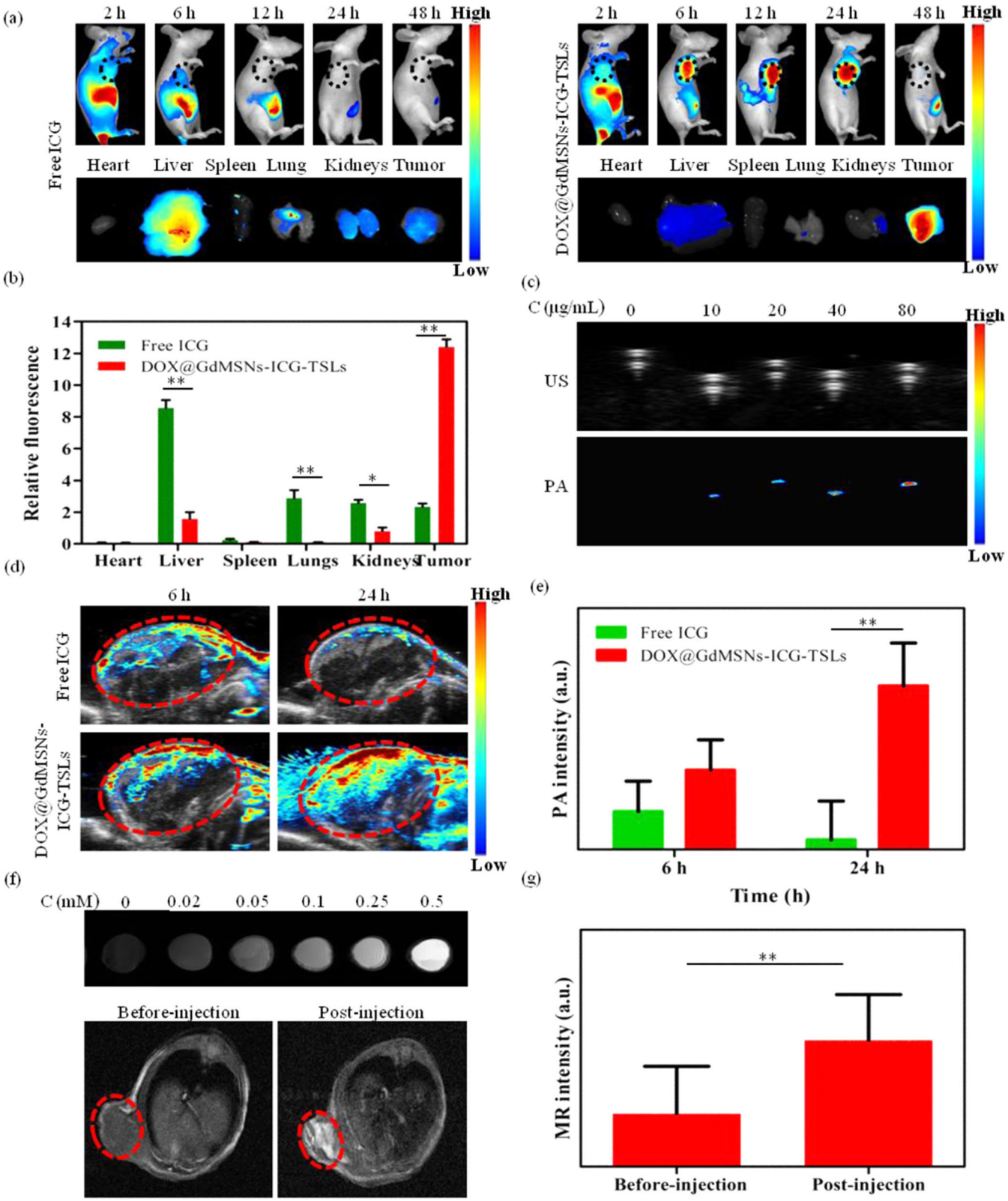


interval debulking, or recurrent ovarian cancer surgery (NCT03180307). Surgimab (SGM-101), a fluorescent anti-carcinoembryonic (CEA) monoclonal antibody, is another promising FIGS probe in phase 1 and 2 clinical trials. This probe is currently being investigated for safety and performance in patients with cancer of the colon, rectum, or

pancreas (NCT02973672). Results from this study suggested that the SGM-101 probe was safe and efficacious in detecting cancer [168]. A recently completed clinical trial investigated the ability of the LUM imaging system and the LUM015 to detect residual breast cancer and reduce positive margins (NCT02438358). The LUM015 probe contains a Cy5 fluorophore linked to a cathepsin activatable peptide. This probe and the LUM imaging system are in several upcoming and currently recruiting clinical trials including a phase C clinical trial for residual breast cancer (NCT03321929), a phase 1/2 study for detection of gastrointestinal cancers (NCT02584244), and a feasibility study for detection of prostate cancer (NCT03441464). The significant increase in clinical trials for FIGS suggests the potential for more rapid regulatory approval and clinical implementation in the future.

## Opportunities in Image-Guided Surgery

FIGS has emerged as an imaging technology with significant potential for clinical efficacy, especially in the field of surgical oncology. Despite its progress, there are still many opportunities for growth in the field. Given below are a few potential examples:

- *Multimodal imaging*: Using a combination of several imaging modalities to diagnose a patient increases diagnostic accuracy. Several recent studies investigated the use of targeted nanoparticles for MRI and FIGS, providing the surgeon concurrence between preoperative planning and intraoperative resection [169, 170]. Combining photoacoustic imaging with FIGS is another area of interest for multimodal imaging [171]. It has been demonstrated that the use of multiple imaging modalities has a synergistic effect on the ability to detect and differentiate cancer both preoperatively and intraoperatively [172].
- *Photodynamic therapy*: FIGS has theranostic capabilities, especially with using NIR contrast agents to induce an immune, chemical, or thermal response in cancer cells. Recent photoimmunotherapy to induce immunogenic cell death with an antibody-conjugated NIR dye has demonstrated an interesting theranostic path to further investigate [173, 174]. Moreover, early studies have begun to explore photodynamic therapy and photothermal therapy as combined imaging and therapy strategies for cancer treatment [175, 176] (Fig. 6).
- *NIR II window*: Typical NIR probes fall in the range of 700–1000 nm, whereas NIR-II agents emit in the 1000–1700 nm range. This shift in emission spectra has demonstrated deeper light penetration depths as well as higher contrast. These preliminary successes suggest a need for further NIR-II probe development [177, 178].
- *Nanotechnology*: Nanotechnology continues to play a key role in FIGS, and offers significant opportunities in terms of conjugation, targeting, and dye encapsulation for enhanced FIGS and multimodality performance. Current research has begun to explore the use of biodegradable nanoparticles for imaging and therapy in cancer treatment [179, 180]. Success in these experiments tackles the concern of toxicity of non-biodegradable nanoparticles, strengthening their potential for translation [150, 151].
- *Refinement of imaging probes*: Further refinement of contrast agents and bulky passive, active, and activatable probes for FIGS is essential to provide the precision and clarity necessary for clinical translation.
- *Applications in advanced cancer models*: In order to apply FIGS technology to highly metastatic and advanced cancers like pancreatic and ovarian, the discovery of early detection biomarkers to target is of utmost importance. Furthermore, the use of large animal models and comparative studies on companion animals as part of standard veterinary treatment may be beneficial.

As FIGS technology progresses, so does the conversation of surgical resection in surgical oncology. In the interest of providing the most comprehensive and precise patient care, FIGS may eventually align with the implementation of highly personalized medicine. The future of FIGS may involve isolating specific cancer biomarkers for a patient, and selecting the corresponding targeted fluorescence probe that would most effectively detect their cancer and metastases. Increased probe specificity and functionality would allow for more complete and thus potentially curative surgical resections for many cancer types. Though many opportunities for growth in the field still exist, FIGS has the potential for widespread implementation as a critical tool for improving surgical resection of cancer.

*Acknowledgements.* This work was supported in part by the National Institutes of Health [grant numbers R01EB019449, R00CA153916, P20 GM103480, and P30CA036727 (Fred and Pamela Buffett Cancer Center at UNMC)], the Nebraska Cattlemen's Ball Development Fund, and the Nebraska Research Initiative.

**Compliance with Ethical Standards**

*Conflict of Interest*

A.M.M. is a co-inventor of image-guided surgery technology that is licensed to Spectropath, Inc. (Atlanta, GA).

## References

1. Stewart B, Wild C (2014) World cancer report 2014. International Agency for Research on Cancer
2. Siegel RL, Miller KD, Jemal A (2018) Cancer statistics, 2018. CA Cancer J Clin 68:7–30
3. Orosco RK, Tsien RY, Nguyen QT (2013) Fluorescence imaging in surgery. IEEE Rev Biomed Eng 6:178–187
4. Nguyen QT, Tsien RY (2013) Fluorescence-guided surgery with live molecular navigation—a new cutting edge. Nat Rev Cancer 13:653–662
5. Keating J, Tchou J, Okusanya O, Fisher C, Batiste R, Jiang J, Kennedy G, Nie S, Singhal S (2016) Identification of breast cancer

margins using intraoperative near-infrared imaging. J Surg Oncol 113:508–514
6. Madajewski B, Judy BF, Mouchli A, Kapoor V, Holt D, Wang MD, Nie S, Singhal S (2012) Intraoperative near-infrared imaging of surgical wounds after tumor resections can detect residual disease. Clin Cancer Res 18:5741–5751
7. Narod S (2016) Can advanced-stage ovarian cancer be cured? Nat Rev Clin Oncol 13:255–261
8. Witkowski ER, Smith JK, Tseng JF (2013) Outcomes following resection of pancreatic cancer. J Surg Oncol 107:97–103
9. Shaib Y, Davila J, Naumann C, El-Serag H (2007) The impact of curative intent surgery on the survival of pancreatic Cancer patients: a U.S. population-based study. Am J Gastroenterol 102:1377–1382
10. Rossi ML, Rehman AA, Gondi CS (2014) Therapeutic options for the management of pancreatic cancer. World J Gastroenterol 20:11142–11159
11. Tamburrino D, Partelli S, Crippa S, Manzoni A, Maurizi A, Falconi M (2014) Selection criteria in resectable pancreatic cancer: a biological and morphological approach. World J Gastroenterol 20:11210–11215
12. Hidalgo M (2010) Pancreatic Cancer. N Engl J Med 362:1605–1617
13. Nick AM, Coleman RL, Ramirez PT, Sood AK (2015) A framework for a personalized surgical approach to ovarian cancer. Nat Rev Clin Oncol 12:239–245
14. Sehouli J, Grabowski JP (2017) Surgery for recurrent ovarian cancer: options and limits. Best Pract Res Clin Obstet Gynaecol 41:88–95
15. Liberale G, Vankerckhove S, Gomez Caldon M et al (2016) Fluorescence imaging after indocyanine green injection for detection of peritoneal metastases in patients undergoing cytoreductive surgery for peritoneal carcinomatosis from colorectal cancer: a pilot study. Ann Surg 264:1110–1115
16. Hoogstins CE, Weixler B, Boogerd LS et al (2017) In search for optimal targets for intraoperative fluorescence imaging of peritoneal metastasis from colorectal cancer. Biomark Cancer 9:1179299X1772825
17. Barth CW, Gibbs SL (2017) Direct administration of nerve-specific contrast to improve nerve sparing radical prostatectomy. Theranostics 7:573–593
18. Gibbs-Strauss SL, Nasr K, Fish KM, Khullar O, Ashitate Y, Siclovan TM, Johnson BF, Barnhardt NE, Tan Hehir CA, Frangioni JV (2011) Nerve-highlighting fluorescent contrast agents for image-guided surgery. Mol Imaging 10:91–101
19. Hussain T, Mastrodimos MB, Raju SC, Glasgow HL, Whitney M, Friedman B, Moore JD, Kleinfeld D, Steinbach P, Messer K, Pu M, Tsien RY, Nguyen QT (2015) Fluorescently labeled peptide increases identification of degenerated facial nerve branches during surgery and improves functional outcome. PLoS One 10:e0119600
20. Hussain T, Nguyen LT, Whitney M, Hasselmann J, Nguyen QT (2016) Improved facial nerve identification during parotidectomy with fluorescently labeled peptide. Laryngoscope 126:2711–2717
21. Whitney MA, Crisp JL, Nguyen LT, Friedman B, Gross LA, Steinbach P, Tsien RY, Nguyen QT (2011) Fluorescent peptides highlight peripheral nerves during surgery in mice. Nat Biotechnol 29:352–356
22. He K, Zhou J, Yang F, Chi C, Li H, Mao Y, Hui B, Wang K, Tian J, Wang J (2018) Near-infrared intraoperative imaging of thoracic sympathetic nerves: from preclinical study to clinical trial. Theranostics 8:304–313
23. Hong G, Antaris AL, Dai H (2017) Near-infrared fluorophores for biomedical imaging. Nat Biomed Eng 1:10
24. Ferraro N, Barbarite E, Albert TR, Berchmans E, Shah AH, Bregy A, Ivan ME, Brown T, Komotar RJ (2016) The role of 5-aminolevulinic acid in brain tumor surgery: a systematic review. Neurosurg Rev 39:545–555
25. Zhao S, Wu J, Wang C, Liu H, Dong X, Shi C, Shi C, Liu Y, Teng L, Han D, Chen X, Yang G, Wang L, Shen C, Li H (2013) Intraoperative fluorescence-guided resection of high-grade malignant gliomas using 5-aminolevulinic acid–induced porphyrins: a systematic review and meta-analysis of prospective studies. PLoS One 8:e63682
26. Hadjipanayis CG, Widhalm G, Stummer W (2015) What is the surgical benefit of utilizing 5-aminolevulinic acid for fluorescence-guided surgery of malignant gliomas? Neurosurgery 77:663–673
27. Moiyadi A, Syed P, Srivastava S (2014) Fluorescence-guided surgery of malignant gliomas based on 5-aminolevulinic acid: paradigm shifts but not a panacea. Nat Rev Cancer 14:146–146
28. Stummer W, Novotny A, Stepp H, Goetz C, Bise K, Reulen HJ (2000) Fluorescence-guided resection of glioblastoma multiforme utilizing 5-ALA-induced porphyrins: a prospective study in 52 consecutive patients. J Neurosurg 93:1003–1013
29. Stummer W, Tonn J-C, Goetz C, Ullrich W, Stepp H, Bink A, Pietsch T, Pichlmeier U (2014) 5-Aminolevulinic acid-derived tumor fluorescence: the diagnostic accuracy of visible fluorescence qualities as corroborated by spectrometry and histology and postoperative imaging. Neurosurgery 74:310–319 20
30. Thevarajah S, Huston TL, Simmons RM (2005) A comparison of the adverse reactions associated with isosulfan blue versus methylene blue dye in sentinel lymph node biopsy for breast cancer. Am J Surg 189:236–239
31. Kidd SA, Lancaster PAL, Anderson JC et al (1996) Fetal death after exposure to methylene blue dye during mid-trimester amniocentesis in twin pregnancy. Prenat Diagn 16:39–47
32. Zhang RR, Schroeder AB, Grudzinski JJ, Rosenthal EL, Warram JM, Pinchuk AN, Eliceiri KW, Kuo JS, Weichert JP (2017) Beyond the margins: real-time detection of cancer using targeted fluorophores. Nat Rev Clin Oncol 14:347–364
33. Verbeek FPR, van der Vorst JR, Schaafsma BE, Swijnenburg RJ, Gaarenstroom KN, Elzevier HW, van de Velde CJH, Frangioni JV, Vahrmeijer AL (2013) Intraoperative near infrared fluorescence guided identification of the ureters using low dose methylene blue: a first in human experience. J Urol 190:574–579
34. Dip FD, Moreira Grecco AD, Nguyen D, Sarotto L, Perrins S, Rosenthal RJ (2015) Ureter identification using methylene blue and fluorescein. In: Fluorescence imaging for surgeons. Springer International Publishing, Cham, pp 327–332
35. Seif C, Martínez Portillo FJ, Osmonov DK, Böhler G, van der Horst C, Leissner J, Hohenfellner R, Juenemann KP, Braun PM (2004) Methylene blue staining for nerve-sparing operative procedures: an animal model. Urology 63:1205–1208
36. Osorio JA, Breshears JD, Arnaout O, Simon NG, Hastings-Robinson AM, Aleshi P, Kliot M (2015) Ultrasound-guided percutaneous injection of methylene blue to identify nerve pathology and guide surgery. Neurosurg Focus 39:E2
37. Candell L, Campbell MJ, Shen WT, Gosnell JE, Clark OH, Duh QY (2014) Ultrasound-guided methylene blue dye injection for parathyroid localization in the reoperative neck. World J Surg 38:88–91
38. Kir G, Alimoglu O, Sarbay BC, Bas G (2014) Ex vivo intra-arterial methylene blue injection in the operation theater may improve the detection of lymph node metastases in colorectal cancer. Pathol Res Pract 210:818–821
39. Tummers QRJG, Schepers A, Hamming JF, Kievit J, Frangioni JV, van de Velde CJH, Vahrmeijer AL (2015) Intraoperative guidance in parathyroid surgery using near-infrared fluorescence imaging and low-dose methylene blue. Surgery 158:1323–1330
40. van der Vorst JR, Schaafsma BE, Verbeek FPR, Swijnenburg RJ, Tummers QRJG, Hutteman M, Hamming JF, Kievit J, Frangioni JV, van de Velde CJH, Vahrmeijer AL (2014) Intraoperative near-infrared fluorescence imaging of parathyroid adenomas with use of low-dose methylene blue. Head Neck 36:853–858
41. van der Vorst JR, Vahrmeijer AL, Hutteman M, Bosse T, Smit VT, van de Velde C, Frangioni JV, Bonsing BA (2012) Near-infrared fluorescence imaging of a solitary fibrous tumor of the pancreas using methylene blue. World J Gastrointest Surg 4:180–184
42. Chu M, Wan Y (2009) Sentinel lymph node mapping using near-infrared fluorescent methylene blue. J Biosci Bioeng 107:455–459
43. Schaafsma BE, Mieog JSD, Hutteman M, van der Vorst JR, Kuppen PJK, Löwik CWGM, Frangioni JV, van de Velde CJH, Vahrmeijer AL (2011) The clinical use of indocyanine green as a near-infrared fluorescent contrast agent for image-guided oncologic surgery. J Surg Oncol 104:323–332
44. Marshall MV, Rasmussen JC, Tan I-C, Aldrich MB, Adams KE, Wang X, Fife CE, Maus EA, Smith LA, Sevick-Muraca EM (2010) Near-infrared fluorescence imaging in humans with Indocyanine green: a review and update. Open Surg Oncol J 2:12–25
45. Namikawa T, Sato T, Hanazaki K (2015) Recent advances in near-infrared fluorescence-guided imaging surgery using indocyanine green. Surg Today 45:1467–1474
46. Pitsinis V, Provenzano E, Kaklamanis L, Wishart GC, Benson JR (2015) Indocyanine green fluorescence mapping for sentinel lymph node biopsy in early breast cancer. Surg Oncol 24:375–379

47. Sugie T, Kassim KA, Takeuchi M, Hashimoto T, Yamagami K, Masai Y, Toi M (2010) A novel method for sentinel lymph node biopsy by indocyanine green fluorescence technique in breast cancer. Cancers (Basel) 2:713–720
48. Vahrmeijer AL, Hutteman M, van der Vorst JR, van de Velde CJH, Frangioni JV (2013) Image-guided cancer surgery using near-infrared fluorescence. Nat Rev Clin Oncol 10:507–518
49. Hill TK, Abdulahad A, Kelkar SS, Marini FC, Long TE, Provenzale JM, Mohs AM (2015) Indocyanine green-loaded nanoparticles for image-guided tumor surgery. Bioconjug Chem 26:294–303
50. Kraft JC, Ho RJY (2014) Interactions of Indocyanine green and lipid in enhancing near-infrared fluorescence properties: the basis for near-infrared imaging *in Vivo*. Biochemistry 53:1275–1283
51. Moore LS, Rosenthal EL, Chung TK, de Boer E, Patel N, Prince AC, Korb ML, Walsh EM, Young ES, Stevens TM, Withrow KP, Morlandt AB, Richman JS, Carroll WR, Zinn KR, Warram JM (2017) Characterizing the utility and limitations of repurposing an open-field optical imaging device for fluorescence-guided surgery in head and neck Cancer patients. J Nucl Med 58:246–251
52. Korb ML, Hartman YE, Kovar J et al (2014) Use of monoclonal antibody-IRDye800CW bioconjugates in the resection of breast cancer HHS public access. J Surg Res 111:119–128
53. Rosenthal EL, Warram JM, de Boer E, Chung TK, Korb ML, Brandwein-Gensler M, Strong TV, Schmalbach CE, Morlandt AB, Agarwal G, Hartman YE, Carroll WR, Richman JS, Clemons LK, Nabell LM, Zinn KR (2015) Safety and tumor specificity of cetuximab-IRDye800 for surgical navigation in head and neck cancer. Clin Cancer Res 21:3658–3666
54. Tansi FL, Rüger R, Rabenhold M, et al (2015) Fluorescence-quenching of a liposomal-encapsulated near-infrared fluorophore as a tool for in vivo optical imaging. J Vis Exp e52136
55. Lisy M-R, Goermar A, Thomas C, Pauli J, Resch-Genger U, Kaiser WA, Hilger I (2008) *In vivo* near-infrared fluorescence imaging of carcinoembryonic antigen–expressing tumor cells in mice. Radiology 247:779–787
56. Pauli J, Brehm R, Spieles M, Kaiser WA, Hilger I, Resch-Genger U (2010) Novel fluorophores as building blocks for optical probes for *in vivo* near infrared fluorescence (NIRF) imaging. J Fluoresc 20:681–693
57. Luo S, Zhang E, Su Y, Cheng T, Shi C (2011) A review of NIR dyes in cancer targeting and imaging. Biomaterials 32:7127–7138
58. Pansare VJ, Hejazi S, Faenza WJ, Prud'homme RK (2012) Review of long-wavelength optical and NIR imaging materials: contrast agents, fluorophores, and multifunctional nano carriers. Chem Mater 24:812–827
59. Lu Y, Su Y, Zhou Y, et al (2013) *In vivo* behavior of near infrared-emitting quantum dots. doi: https://doi.org/10.1016/j.biomaterials.2013.02.054
60. Moore GE, Peyton WT, French LA, Walker WW (1948) The clinical use of fluorescein in neurosurgery. J Neurosurg 5:392–398
61. Dilek O, Ihsan A, Tulay H (2011) Anaphylactic reaction after fluorescein sodium administration during intracranial surgery. J Clin Neurosci 18:430–431
62. Tanahashi S, Iida H, Dohi S (1995) An anaphylactoid reaction after administration of fluorescein sodium during neurosurgery. Can J Anaesth 42:181–185
63. Mondal SB, Gao S, Zhu N et al (2014) Real-time fluorescence image-guided oncologic surgery. Adv Cancer Res 124:171–211
64. Ji X, Peng F, Zhong Y, Su Y, He Y (2014) Fluorescent quantum dots: synthesis, biomedical optical imaging, and biosafety assessment. Colloids Surfaces B Biointerfaces 124:132–139
65. Smith AM, Duan H, Mohs AM, Nie S (2008) Bioconjugated quantum dots for *in vivo* molecular and cellular imaging. Adv Drug Deliv Rev 60:1226–1240
66. Hill TK, Mohs AM (2016) Image-guided tumor surgery: will there be a role for fluorescent nanoparticles? Wiley Interdiscip Rev Nanomed Nanobiotechnol 8:498–511
67. Gioux S, Kianzad V, Ciocan R, Gupta S, Oketokoun R, Frangioni JV (2009) High-power, computer-controlled, light-emitting diode-based light sources for fluorescence imaging and image-guided surgery. Mol Imaging 8:156–165
68. Gioux S, Choi HS, Frangioni JV (2010) Image-guided surgery using invisible near-infrared light: fundamentals of clinical translation. Mol Imaging 9:237–255
69. DSouza AV, Lin H, Henderson ER, Samkoe KS, Pogue BW (2016) Review of fluorescence guided surgery systems: identification of key performance capabilities beyond indocyanine green imaging. J Biomed Opt 21:80901
70. Zhu B, Sevick-Muraca EM (2015) A review of performance of near-infrared fluorescence imaging devices used in clinical studies. Br J Radiol 88:20140547
71. Matsumura Y, Maeda H, Jain RK et al (1986) A new concept for macromolecular therapeutics in cancer chemotherapy: mechanism of tumoritropic accumulation of proteins and the antitumor agent smancs. Cancer Res 46:6387–6392
72. Bertrand N, Wu J, Xu X, Kamaly N, Farokhzad OC (2014) Cancer nanotechnology: the impact of passive and active targeting in the era of modern cancer biology. Adv Drug Deliv Rev 66:2–25
73. Maeda H, Tsukigawa K, Fang J (2016) A retrospective 30 years after discovery of the enhanced permeability and retention effect of solid tumors: next-generation chemotherapeutics and photodynamic therapy-problems, solutions, and prospects. Microcirculation 23:173–182
74. Kharaishvili G, Simkova D, Bouchalova K, Gachechiladze M, Narsia N, Bouchal J (2014) The role of cancer-associated fibroblasts, solid stress and other microenvironmental factors in tumor progression and therapy resistance. Cancer Cell Int 14:41
75. Fang J, Nakamura H, Maeda H (2011) The EPR effect: unique features of tumor blood vessels for drug delivery, factors involved, and limitations and augmentation of the effect. Adv Drug Deliv Rev 63:136–151
76. Carmeliet P, Jain RK (2000) Angiogenesis in cancer and other diseases. Nature 407:249–257
77. Bergers G, Benjamin LE (2003) Angiogenesis: tumorigenesis and the angiogenic switch. Nat Rev Cancer 3:401–410
78. Morikawa S, Baluk P, Kaidoh T, Haskell A, Jain RK, McDonald DM (2002) Abnormalities in pericytes on blood vessels and endothelial sprouts in tumors. Am J Pathol 160:985–1000
79. Padera TP, Kadambi A, di Tomaso E, Carreira CM, Brown EB, Boucher Y, Choi NC, Mathisen D, Wain J, Mark EJ, Munn LL, Jain RK (2002) Lymphatic metastasis in the absence of functional intratumor lymphatics. Science 296:1883–1886
80. Sriraman SK, Aryasomayajula B, Torchilin VP (2014) Barriers to drug delivery in solid tumors. Tissue Barriers 2:e29528
81. Maeda H (2012) Macromolecular therapeutics in cancer treatment: the EPR effect and beyond. J Control Release 164:138–144
82. Nakamura H, Etrych T, Chytil P, Ohkubo M, Fang J, Ulbrich K, Maeda H (2014) Two step mechanisms of tumor selective delivery of N-(2-hydroxypropyl)methacrylamide copolymer conjugated with pirarubicin via an acid-cleavable linkage. J Control Release 174:81–87
83. Kobayashi H, Watanabe R, Choyke PL (2013) Improving conventional enhanced permeability and retention (EPR) effects; what is the appropriate target? Theranostics 4:81–89
84. Nakamura Y, Mochida A, Choyke PL, Kobayashi H (2016) Nanodrug delivery: is the enhanced permeability and retention effect sufficient for curing cancer? Bioconjug Chem 27:2225–2238
85. Jain RK, Stylianopoulos T (2010) Delivering nanomedicine to solid tumors. Nat Rev Clin Oncol 7:653–664
86. Padera TP, Stoll BR, Tooredman JB, Capen D, Tomaso E, Jain RK (2004) Pathology: cancer cells compress intratumour vessels. Nature 427:695–695
87. Jain RK, Martin JD, Stylianopoulos T (2014) The role of mechanical forces in tumor growth and therapy. Annu Rev Biomed Eng 16:321–346
88. Heldin C-H, Rubin K, Pietras K, Östman A (2004) High interstitial fluid pressure — an obstacle in cancer therapy. Nat Rev Cancer 4:806–813
89. Baxter LT, Jain' RK (1989) Transport of fluid and macromolecules in tumors I. Role of interstitial pressure and convection. Microvasc Res 37:77–104
90. Wu M, Frieboes HB, Chaplain MAJ, McDougall SR, Cristini V, Lowengrub JS (2014) The effect of interstitial pressure on therapeutic agent transport: coupling with the tumor blood and lymphatic vascular systems. J Theor Biol 355:194–207
91. Miao L, Lin CM, Huang L (2015) Stromal barriers and strategies for the delivery of nanomedicine to desmoplastic tumors. J Control Release 219:192–204

92. May JP, Li S-D (2013) Hyperthermia-induced drug targeting. Expert Opin Drug Deliv 10:511–527
93. Durymanov MO, Rosenkranz AA, Sobolev AS (2015) Current approaches for improving Intratumoral accumulation and distribution of nanomedicines. Theranostics 5:1007–1020
94. Ojha T, Pathak V, Shi Y, et al (2017) Pharmacological and physical vessel modulation strategies to improve EPR-mediated drug targeting to tumors. Advanced Drug Delivery Reviews 119:44–60
95. Yokoi K, Tanei T, Godin B, van de Ven AL, Hanibuchi M, Matsunoki A, Alexander J, Ferrari M (2014) Serum biomarkers for personalization of nanotherapeutics-based therapy in different tumor and organ microenvironments. Cancer Lett 345:48–55
96. Yokoi K, Kojic M, Milosevic M, Tanei T, Ferrari M, Ziemys A (2014) Capillary-wall collagen as a biophysical marker of nanotherapeutic permeability into the tumor microenvironment. Cancer Res 74:4239–4246
97. Bolkestein M, de Blois E, Koelewijn SJ, Eggermont AMM, Grosveld F, de Jong M, Koning GA (2016) Investigation of factors determining the enhanced permeability and retention effect in subcutaneous xenografts. J Nucl Med 57:601–607
98. Miller J, Wang ST, Orukari I, Prior J, Sudlow G, Su X, Liang K, Tang R, Hillman EMC, Weilbaecher KN, Culver JP, Berezin MY, Achilefu S (2017) Perfusion-based fluorescence imaging method delineates diverse organs and identifies multifocal tumors using generic near infrared molecular probes. J Biophotonics 11:e201700232. https://doi.org/10.1002/jbio.201700232
99. Srinivasarao M, Galliford CV, Low PS (2015) Principles in the design of ligand-targeted cancer therapeutics and imaging agents. Nat Rev Drug Discov 14:203–219
100. Choi HS, Gibbs SL, Lee JH, Kim SH, Ashitate Y, Liu F, Hyun H, Park GL, Xie Y, Bae S, Henary M, Frangioni JV (2013) Targeted zwitterionic near-infrared fluorophores for improved optical imaging. Nat Biotechnol 31:148–153
101. Nagaya T, Nakamura YA, Choyke PL, Kobayashi H (2017) Fluorescence-guided surgery. Front Oncol 7:314
102. Warram JM, de Boer E, Sorace AG, Chung TK, Kim H, Pleijhuis RG, van Dam GM, Rosenthal EL (2014) Antibody-based imaging strategies for cancer. Cancer Metastasis Rev 33:809–822
103. Hiroshima Y, Lwin TM, Murakami T, Mawy AA, Kuniya T, Chishima T, Endo I, Clary BM, Hoffman RM, Bouvet M (2016) Effective fluorescence-guided surgery of liver metastasis using a fluorescent anti-CEA antibody. J Surg Oncol 114:951–958
104. Lwin TM, Murakami T, Miyake K et al (2018) Tumor-specific labeling of pancreatic cancer using a humanized anti-CEA antibody conjugated to a near-infrared fluorophore. Ann Surg Oncol:1–7
105. Moore LS, Rosenthal EL, de Boer E, Prince AC, Patel N, Richman JM, Morlandt AB, Carroll WR, Zinn KR, Warram JM (2017) Effects of an unlabeled loading dose on tumor-specific uptake of a fluorescently labeled antibody for optical surgical navigation. Mol Imaging Biol 19:610–616
106. Freise AC, Wu AM (2015) *In vivo* imaging with antibodies and engineered fragments. Mol Immunol 67:142–152
107. Kobayashi H, Choyke PL, Ogawa M (2016) Monoclonal antibody-based optical molecular imaging probes; considerations and caveats in chemistry, biology and pharmacology. Curr Opin Chem Biol 33:32–38
108. Mazzocco C, Fracasso G, Germain-Genevois C, Dugot-Senant N, Figini M, Colombatti M, Grenier N, Couillaud F (2016) *In vivo* imaging of prostate cancer using an anti-PSMA scFv fragment as a probe. Sci Rep 6:23314
109. Sonn GA, Behesnilian AS, Jiang ZK, Zettlitz KA, Lepin EJ, Bentolila LA, Knowles SM, Lawrence D, Wu AM, Reiter RE (2016) Fluorescent image-guided surgery with an anti-prostate stem cell antigen (PSCA) diabody enables targeted resection of mouse prostate cancer xenografts in real time. Clin Cancer Res 22:1403–1412
110. Owens B (2017) Faster, deeper, smaller—the rise of antibody-like scaffolds. Nat Biotechnol 35:602–603
111. Sexton K, Tichauer K, Samkoe KS, Gunn J, Hoopes PJ, Pogue BW (2013) Fluorescent affibody peptide penetration in glioma margin is superior to full antibody. PLoS One 8:e60390
112. de Souza ALR, Marra K, Gunn J, Samkoe KS, Hoopes PJ, Feldwisch J, Paulsen KD, Pogue BW (2017) Fluorescent affibody molecule administered *in vivo* at a microdose level labels EGFR expressing glioma tumor regions. Mol Imaging Biol 19:41–48
113. Samkoe KS, Gunn JR, Marra K, Hull SM, Moodie KL, Feldwisch J, Strong TV, Draney DR, Hoopes PJ, Roberts DW, Paulsen K, Pogue BW (2017) Toxicity and pharmacokinetic profile for single-dose injection of ABY-029: a fluorescent anti-EGFR synthetic affibody molecule for human use. Mol Imaging Biol 19:512–521
114. Chakravarty R, Goel S, Cai W (2014) Nanobody: the "magic bullet" for molecular imaging? Theranostics 4:386–398
115. Debie P, Vanhoeij M, Poortmans N et al (2017) Improved debulking of peritoneal tumor implants by near-infrared fluorescent nanobody image guidance in an experimental mouse model. Mol Imaging Biol:1–7
116. Staderini M, Megia-Fernandez A, Dhaliwal K, Bradley M (2017) Peptides for optical medical imaging and steps towards therapy. Bioorg Med Chem 26:2816–2826. https://doi.org/10.1016/J.BMC.2017.09.039
117. Sun X, Li Y, Liu T et al (2017) Peptide-based imaging agents for cancer detection. Adv Drug Deliv Rev 110–111:38–51
118. Handgraaf HJM, Boonstra MC, Prevoo HAJM, Kuil J, Bordo MW, Boogerd LSF, Sibinga Mulder BG, Sier CFM, Vinkenburg-van Slooten M, Valentijn ARPM, Burggraaf J, van de Velde C, Frangioni JV, Vahrmeijer AL (2017) Real-time near-infrared fluorescence imaging using cRGD-ZW800-1 for intraoperative visualization of multiple cancer types. Oncotarget 8:21054–21066
119. Sato K, Gorka AP, Nagaya T, Michie MS, Nani RR, Nakamura Y, Coble VL, Vasalatiy OV, Swenson RE, Choyke PL, Schnermann MJ, Kobayashi H (2016) Role of fluorophore charge on the *In Vivo* optical imaging properties of near-infrared cyanine dye/monoclonal antibody conjugates. Bioconjug Chem 27:404–413
120. Yin X, Wang M, Wang H, Deng H, He T, Tan Y, Zhu Z, Wu Z, Hu S, Li Z (2017) Evaluation of neurotensin receptor 1 as a potential imaging target in pancreatic ductal adenocarcinoma. Amino Acids 49:1325–1335
121. Wyatt LC, Lewis JS, Andreev OA, Reshetnyak YK, Engelman DM (2017) Applications of pHLIP technology for cancer imaging and therapy. Trends Biotechnol 35:653–664
122. Golijanin J, Amin A, Moshnikova A, Brito JM, Tran TY, Adochite RC, Andreev GO, Crawford T, Engelman DM, Andreev OA, Reshetnyak YK, Golijanin D (2016) Targeted imaging of urothelium carcinoma in human bladders by an ICG pHLIP peptide ex vivo. Proc Natl Acad Sci U S A 113:11829–11834
123. Karabadzhak AG, An M, Yao L, Langenbacher R, Moshnikova A, Adochite RC, Andreev OA, Reshetnyak YK, Engelman DM (2014) pHLIP-FIRE, a cell insertion-triggered fluorescent probe for imaging tumors demonstrates targeted cargo delivery *in vivo*. ACS Chem Biol 9:2545–2553
124. Darmostuk M, Rimpelova S, Gbelcova H, Ruml T (2015) Current approaches in SELEX: an update to aptamer selection technology. Biotechnol Adv 33:1141–1161
125. Hori S, Herrera A, Rossi J, Zhou J (2018) Current advances in aptamers for cancer diagnosis and therapy. Cancers (Basel) 10:9
126. Huang YF, Chang HT, Tan W (2008) Cancer cell targeting using multiple aptamers conjugated on nanorods. Anal Chem 80:567–572
127. Tang J, Huang N, Zhang X, Zhou T, Tan Y, Pi J, Pi L, Cheng S, Zheng H, Cheng Y (2017) Aptamer-conjugated PEGylated quantum dots targeting epidermal growth factor receptor variant III for fluorescence imaging of glioma. Int J Nanomedicine 12:3899–3911
128. Tan J, Yang N, Zhong L, Tan J, Hu Z, Zhao Q, Gong W, Zhang Z, Zheng R, Lai Z, Li Y, Zhou C, Zhang G, Zheng D, Zhang Y, Wu S, Jiang X, Zhong J, Huang Y, Zhou S, Zhao Y (2017) A new theranostic system based on endoglin aptamer conjugated fluorescent silica nanoparticles. Theranostics 7:4862–4876
129. Bazak R, Houri M, El Achy S et al (2015) Cancer active targeting by nanoparticles: a comprehensive review of literature. J Cancer Res Clin Oncol 141:769–784
130. Duman FD, Erkisa M, Khodadust R, Ari F, Ulukaya E, Acar HY (2017) Folic acid-conjugated cationic Ag2S quantum dots for optical imaging and selective doxorubicin delivery to HeLa cells. Nanomedicine 12:2319–2333
131. Predina JD, Newton AD, Connolly C, Dunbar A, Baldassari M, Deshpande C, Cantu E III, Stadanlick J, Kularatne SA, Low PS, Singhal S (2018) Identification of a folate receptor-targeted near-infrared molecular contrast agent to localize pulmonary adenocarcinomas. Mol Ther 26:390–403

132. Hoogstins CES, Tummers QRJG, Gaarenstroom KN, de Kroon CD, Trimbos JBMZ, Bosse T, Smit VTHBM, Vuyk J, van de Velde CJH, Cohen AF, Low PS, Burggraaf J, Vahrmeijer AL (2016) A novel tumor-specific agent for intraoperative near-infrared fluorescence imaging: a translational study in healthy volunteers and patients with ovarian cancer. Clin Cancer Res 22:2929–2938
133. Keating JJ, Runge JJ, Singhal S, Nims S, Venegas O, Durham AC, Swain G, Nie S, Low PS, Holt DE (2017) Intraoperative near-infrared fluorescence imaging targeting folate receptors identifies lung cancer in a large-animal model. Cancer 123:1051–1060
134. Zhu M, Sheng Z, Jia Y, Hu D, Liu X, Xia X, Liu C, Wang P, Wang X, Zheng H (2017) Indocyanine green-holo-transferrin nanoassemblies for tumor-targeted dual-modal imaging and photothermal therapy of glioma. ACS Appl Mater Interfaces 9:39249–39258
135. Mochida A, Ogata F, Nagaya T, Choyke PL, Kobayashi H (2018) Activatable fluorescent probes in fluorescence-guided surgery: practical considerations. Bioorg Med Chem 26:925–930
136. Kobayashi H, Choyke PL (2011) Target-cancer-cell-specific activatable fluorescence imaging probes: rational design and *in vivo* applications. Acc Chem Res 44:83–90
137. Chinen AB, Guan CM, Ferrer JR, Barnaby SN, Merkel TJ, Mirkin CA (2015) Nanoparticle probes for the detection of cancer biomarkers, cells, and tissues by fluorescence. Chem Rev 115:10530–10574
138. Choi HS, Liu W, Liu F, Nasr K, Misra P, Bawendi MG, Frangioni JV (2010) Design considerations for tumour-targeted nanoparticles. Nat Nanotechnol 5:42–47
139. Chi C, Zhang Q, Mao Y, Kou D, Qiu J, Ye J, Wang J, Wang Z, du Y, Tian J (2015) Increased precision of orthotopic and metastatic breast cancer surgery guided by matrix metalloproteinase-activatable near-infrared fluorescence probes. Sci Rep 5:14197
140. Alley SC, Okeley NM, Senter PD (2010) Antibody–drug conjugates: targeted drug delivery for cancer. Curr Opin Chem Biol 14:529–537
141. Matsuzaki S, Serada S, Hiramatsu K, Nojima S, Matsuzaki S, Ueda Y, Ohkawara T, Mabuchi S, Fujimoto M, Morii E, Yoshino K, Kimura T, Naka T (2018) Anti-glypican-1 antibody-drug conjugate exhibits potent preclinical antitumor activity against glypican-1 positive uterine cervical cancer. Int J Cancer 142:1056–1066
142. Su C-Y, Chen M, Chen L-C, Ho YS, Ho HO, Lin SY, Chuang KH, Sheu MT (2018) Bispecific antibodies (anti-mPEG/anti-HER2) for active tumor targeting of docetaxel (DTX)-loaded mPEGylated nanocarriers to enhance the chemotherapeutic efficacy of HER2-overexpressing tumors. Drug Deliv 25:1066–1079
143. Semkina AS, Abakumov MA, Skorikov AS, Abakumova TO, Melnikov PA, Grinenko NF, Cherepanov SA, Vishnevskiy DA, Naumenko VA, Ionova KP, Majouga AG, Chekhonin VP (2018) Multimodal doxorubicin loaded magnetic nanoparticles for VEGF targeted theranostics of breast cancer. Nanomedicine 14:1733–1742. https://doi.org/10.1016/j.nano.2018.04.019
144. Huang R, Li J, Kebebe D, Wu Y, Zhang B, Liu Z (2018) Cell penetrating peptides functionalized gambogic acid-nanostructured lipid carrier for cancer treatment. Drug Deliv 25:757–765
145. Deshpande P, Jhaveri A, Pattni B, Biswas S, Torchilin V (2018) Transferrin and octaarginine modified dual-functional liposomes with improved cancer cell targeting and enhanced intracellular delivery for the treatment of ovarian cancer. Drug Deliv 25:517–532
146. Alibolandi M, Ramezani M, Abnous K, Hadizadeh F (2016) AS1411 aptamer-decorated biodegradable polyethylene glycol–poly(lactic-co-glycolic acid) nanopolymersomes for the targeted delivery of gemcitabine to non–small cell lung cancer *in vitro*. J Pharm Sci 105:1741–1750
147. Lin R, Huang J, Wang L, Li Y, Lipowska M, Wu H, Yang J, Mao H (2018) Bevacizumab and near infrared probe conjugated iron oxide nanoparticles for vascular endothelial growth factor targeted MR and optical imaging. Biomater Sci 6:1517–1525. https://doi.org/10.1039/C8BM00225H
148. Rijpkema M, Oyen WJ, Bos D, Franssen GM, Goldenberg DM, Boerman OC (2014) SPECT- and fluorescence image-guided surgery using a dual-labeled carcinoembryonic antigen-targeting antibody. J Nucl Med 55:1519–1524
149. Zhang X-S, Xuan Y, Yang X-Q, Cheng K, Zhang RY, Li C, Tan F, Cao YC, Song XL, An J, Hou XL, Zhao YD (2018) A multifunctional targeting probe with dual-mode imaging and photothermal therapy used *in vivo*. J Nanobiotechnology 16:42
150. Yang H-M, Park CW, Park S, Kim J-D (2018) Cross-linked magnetic nanoparticles with a biocompatible amide bond for cancer-targeted dual optical/magnetic resonance imaging. Colloids Surf B Biointerfaces 161:183–191
151. Kommidi H, Guo H, Nurili F, Vedvyas Y, Jin MM, McClure TD, Ehdaie B, Sayman HB, Akin O, Aras O, Ting R (2018) $^{18}$F-positron emitting/trimethine cyanine-fluorescent contrast for image-guided prostate cancer management. J Med Chem 61:4256–4262
152. Wang X, Yan J, Pan D, et al (2018) Polyphenol-poloxamer self-assembled supramolecular nanoparticles for tumor NIRF/PET imaging. Adv Healthc Mater 15:1701505
153. Chi C, Du Y, Ye J et al (2014) Intraoperative imaging-guided cancer surgery: from current fluorescence molecular imaging methods to future multi-modality imaging technology. Theranostics 4:1072–1084
154. Hausner SH, Bauer N, Hu LY, Knight LM, Sutcliffe JL (2015) The effect of bi-terminal PEGylation of an integrin $\alpha v\beta_6$-targeted $^{18}$F peptide on pharmacokinetics and tumor uptake. J Nucl Med 56:784–790
155. Han Z, Li Y, Roelle S, Zhou Z, Liu Y, Sabatelle R, DeSanto A, Yu X, Zhu H, Magi-Galluzzi C, Lu ZR (2017) Targeted contrast agent specific to an oncoprotein in tumor microenvironment with the potential for detection and risk stratification of prostate cancer with MRI. Bioconjug Chem 28:1031–1040
156. Rosenthal EL, Warram JM, Bland KI, Zinn KR (2015) The status of contemporary image-guided modalities in oncologic surgery. Ann Surg 261:46–55
157. Kim MJ, Kim CS, Park YS et al (2016) The efficacy of intraoperative frozen section analysis during breast-conserving surgery for patients with ductal carcinoma in situ. Breast Cancer (Auckl) 10:205–210
158. Ko S, Chun YK, Kang SS, Hur MH (2017) The usefulness of intraoperative circumferential frozen-section analysis of lumpectomy margins in breast-conserving surgery. J Breast Cancer 20:176–182
159. Pleijhuis RG, Graafland M, de Vries J, Bart J, de Jong JS, van Dam GM (2009) Obtaining adequate surgical margins in breast-conserving therapy for patients with early-stage breast cancer: current modalities and future directions. Ann Surg Oncol 16:2717–2730
160. Petropoulou T, Kapoula A, Mastoraki A et al (2017) Imprint cytology versus frozen section analysis for intraoperative assessment of sentinel lymph node in breast cancer. Breast Cancer (Dove Med Press) 9:325–330
161. Barth CW, Schaefer JM, Rossi VM, Davis SC, Gibbs SL (2017) Optimizing fresh specimen staining for rapid identification of tumor biomarkers during surgery. Theranostics 7:4722–4734
162. Hutteman M, Choi HS, Mieog JSD, van der Vorst JR, Ashitate Y, Kuppen PJK, van Groningen MC, Löwik CWGM, Smit VTHBM, van de Velde CJH, Frangioni JV, Vahrmeijer AL (2011) Clinical translation of ex vivo sentinel lymph node mapping for colorectal cancer using invisible near-infrared fluorescence light. Ann Surg Oncol 18:1006–1014
163. Cutter JL, Cohen NT, Wang J, Sloan AE, Cohen AR, Panneerselvam A, Schluchter M, Blum G, Bogyo M, Basilion JP (2012) Topical application of activity-based probes for visualization of brain tumor tissue. PLoS One 7:e33060
164. Tipirneni KE, Warram JM, Moore LS, Prince AC, de Boer E, Jani AH, Wapnir IL, Liao JC, Bouvet M, Behnke NK, Hawn MT, Poultsides GA, Vahrmeijer AL, Carroll WR, Zinn KR, Rosenthal E (2017) Oncologic procedures amenable to fluorescence-guided surgery. Ann Surg 266:36–47
165. Tummers WS, Warram JM, Tipirneni KE et al (2017) Regulatory aspects of optical methods and exogenous targets for cancer detection. Cancer Res 77:2197 LP–2192206
166. Mondal SB, Gao S, Zhu N et al (2015) Binocular goggle augmented imaging and navigation system provides real-time fluorescence image guidance for tumor resection and sentinel lymph node mapping. Sci Rep 5:12117
167. Mondal SB, Gao S, Zhu N, Habimana-Griffin LM, Akers WJ, Liang R, Gruev V, Margenthaler J, Achilefu S (2017) Optical see-through cancer vision goggles enable direct patient visualization and real-time fluorescence-guided oncologic surgery. Ann Surg Oncol 24:1897–1903

168. Boogerd LSF, Hoogstins CES, Schaap DP, Kusters M, Handgraaf HJM, van der Valk MJM, Hilling DE, Holman FA, Peeters KCMJ, Mieog JSD, van de Velde CJH, Farina-Sarasqueta A, van Lijnschoten I, Framery B, Pèlegrin A, Gutowski M, Nienhuijs SW, de Hingh IHJT, Nieuwenhuijzen GAP, Rutten HJT, Cailler F, Burggraaf J, Vahrmeijer AL (2018) Safety and effectiveness of SGM-101, a fluorescent antibody targeting carcinoembryonic antigen, for intraoperative detection of colorectal cancer: a dose-escalation pilot study. Lancet Gastroenterol Hepatol 3:181–191
169. Payne WM, Hill TK, Svechkarev D, Holmes MB, Sajja BR, Mohs AM (2017) Multimodal imaging nanoparticles derived from hyaluronic acid for integrated preoperative and intraoperative cancer imaging. Contrast Media Mol Imaging 2017:1–14
170. Gao N, Bozeman EN, Qian W, Wang L, Chen H, Lipowska M, Staley CA, Wang YA, Mao H, Yang L (2017) Tumor penetrating theranostic nanoparticles for enhancement of targeted and image-guided drug delivery into peritoneal tumors following intraperitoneal delivery. Theranostics 7:1689–1704
171. Biffi S, Petrizza L, Garrovo C, Rampazzo E, Andolfi L, Giustetto P, Nikolov I, Kurdi G, Danailov MB, Zauli G, Secchiero P, Prodi L (2016) Multimodal near-infrared-emitting PluS silica nanoparticles with fluorescent, photoacoustic, and photothermal capabilities. Int J Nanomedicine 11:4865–4874
172. Lu Z, Pham TT, Rajkumar V, Yu Z, Pedley RB, Årstad E, Maher J, Yan R (2018) A dual reporter iodinated labeling reagent for cancer positron emission tomography imaging and fluorescence-guided surgery. J Med Chem 61:1636–1645
173. Nagaya T, Nakamura Y, Sato K, Harada T, Choyke PL, Hodge JW, Schlom J, Kobayashi H (2017) Near infrared photoimmunotherapy with avelumab, an anti-programmed death-ligand 1 (PD-L1) antibody. Oncotarget 8:8807–8817
174. Maruoka Y, Nagaya T, Nakamura Y, Sato K, Ogata F, Okuyama S, Choyke PL, Kobayashi H (2017) Evaluation of early therapeutic effects after near-infrared Photoimmunotherapy (NIR-PIT) using luciferase–luciferin photon-counting and fluorescence imaging. Mol Pharm 14:4628–4635
175. Sun Q, You Q, Wang J, Liu L, Wang Y, Song Y, Cheng Y, Wang S, Tan F, Li N (2018) Theranostic Nanoplatform: triple-modal imaging-guided synergistic cancer therapy based on liposome-conjugated mesoporous silica nanoparticles. ACS Appl Mater Interfaces 10:1963–1975
176. Li X, Schumann C, Albarqi HA, Lee CJ, Alani AWG, Bracha S, Milovancev M, Taratula O, Taratula O (2018) A tumor-activatable theranostic nanomedicine platform for NIR fluorescence-guided surgery and combinatorial phototherapy. Theranostics 8:767–784
177. Sun Y, Ding M, Zeng X, Xiao Y, Wu H, Zhou H, Ding B, Qu C, Hou W, Er-bu AGA, Zhang Y, Cheng Z, Hong X (2017) Novel bright-emission small-molecule NIR-II fluorophores for *in vivo* tumor imaging and image-guided surgery. Chem Sci 8:3489–3493
178. Cheng K, Chen H, Jenkins CH, Zhang G, Zhao W, Zhang Z, Han F, Fung J, Yang M, Jiang Y, Xing L, Cheng Z (2017) Synthesis, characterization, and biomedical applications of a targeted dual-modal near-infrared-II fluorescence and photoacoustic imaging Nanoprobe. ACS Nano 11:12276–12291
179. Miao W, Kim H, Gujrati V, Kim JY, Jon H, Lee Y, Choi M, Kim J, Lee S, Lee DY, Kang S, Jon S (2016) Photo-decomposable organic nanoparticles for combined tumor optical imaging and multiple phototherapies. Theranostics 6:2367–2379
180. Liu L, Ruan Z, Yuan P, Li T, Yan L (2018) Oxygen self-sufficient amphiphilic polypeptide nanoparticles encapsulating BODIPY for potential near infrared imaging-guided photodynamic therapy at low energy. Nanotheranostics 2:59–69